

A Shoreline Evolution Model with Wave Crest Model on I-Head and T-Head Groin Structures with Different Types of Breaking Wave

Pidok Unyapoti, Nopparat Pochai

Abstract— Beach erosion is a process that results in changes to the materials of a shoreline, with erosion being the removal of material from the shoreline more than its addition. Beach erosion on the shorelines causes loss of landforms and a reduction in size, leading to the need for the development of various structures to mitigate beach erosion. Groin is one of the commonly utilized structures for coastal erosion prevention, and groins of various shapes and forms have been developed to minimize beach erosion to the greatest extent possible. We have focused on assessing the impacts of I-head and T-head groin structures on shoreline evolution, approximated through a shoreline evolution model. Various techniques for setting initial conditions and boundary conditions have been discussed. Additionally, we have explored the structural impacts of these two groin types. We considered the average wave crest impact angle obtained from a wave crest impact model on both the left and right sides of the shoreline, differing over a span of four wavelengths. To estimate shoreline evolution for each year, we employed traditional forward time-centered space techniques and the unconditionally stable Saul'yev finite differential techniques. The results of shoreline evolution calculations for both groin structures were found to be consistent across the four cases of the wave crest impact model.

Index Terms— shoreline evolution, groin structure system, explicit finite difference method, wave crest impact, mathematical model

I. INTRODUCTION

Beach erosion and deposition are significant phenomena that have a profound impact on shorelines. They are caused by the interaction of water levels and waves with the beach, which causes a transfer in the composition of beach sediments like gravel, rocks, and sand. These changes have the potential to alter the shape and profile of the beach. Whether it is residential areas or transportation infrastructure, the problem of beach erosion can have severe consequences and is a common issue faced by many countries.

Consequently, there have been extensive studies to

Manuscript received March 6, 2024; revised March 13, 2024.

This paper is supported by King Mongkut's Institute of Technology Ladkrabang.

N. Pochai is an Associate Professor of Department of Mathematics, Faculty of Science, King Mongkut's Institute of Technology Ladkrabang, Bangkok, 10520, Thailand (corresponding author to provide phone: 662-329-8400; fax: 662-329-8400; e-mail: nop_math@yahoo.com).

P. Unyapoti is a PhD. candidate of Mathematics Department, Faculty of Science, King Mongkut's Institute of Technology Ladkrabang, Bangkok, 10520, Thailand (e-mail: pidokunyapoti@gmail.com).

understand the implications of beach erosion on shorelines. In [1], they proposed a two-step methodology to determining the profile reaction to sea level rise (SLR) in the presence of seawalls, which includes using the profile translation model to calculate the erosion demand and redistributing the eroded volume in front of the seawall to the position of the offshore bar. The erosion demand due to sea level rise (SLR) is the same whether a seawall is there or not; nevertheless, a seawall focuses erosion in the area around it, resulting in aggravated and localized profile erosion. The type of seawall structure had no significant effect on the beach's response to sea level rise (SLR). In [2], they proposed using the Bruun Rule and equilibrium shoreline models to estimate coastal recession caused by sea-level rise (SLR). The incorporation of SLR-driven regression to equilibrium shoreline models is examined, and the physical processes behind the Bruun Rule are fully stated in the integrated model. In [4], they studied and evaluated the effectiveness of existing coastal protection structures in restraining erosion at Padang Beach. The modeling results show that erosion could begin at the Batang Arau river mouth in the absence of protective barriers, with substantial erosion estimated to begin roughly 59.04 meters from the coast. With the presence of coastal protection structures, the model results reveal sedimentation of 7.33 meters of coastal from its initial position, which occurs 475 meters from the border. The study reveals that while groins on Padang beaches appear to be highly effective in maintaining the shoreline's littoral transport direction, their installation does not considerably increase the coastal.

To prevent beach erosion, various methods have been developed to reduce the rate of beach erosion. These methods often involve the construction of different structures aimed at protecting shorelines. Common approaches to mitigating beach erosion include seawalls, breakwaters, groins, etc. In [3], they developed numerical model is validated using a well-known practical test scenario involving a wave train approaching a beach with a T-head groin construction, and the computational and experimental findings are compared in detail. The model's numerical approach resolves the three-dimensional Navier-Stokes equations in a contravariant composition, accounting for a time-dependent coordinate system and shifting vertical coordinates over time to correspond to free-surface altitude. In [6], they predicted the effect of GROPOZAG, a single zigzag-type porous groin, on the change in beach profile. The study looks into the effects of various parameters on

beach erosion and sedimentation, such as groin length, groin orientation, and wave steepness. The experiments were carried out at Syiah Kuala University's Laboratory of River and Coastal Engineering using a small-scale physical model. The results show that zigzag porous groins reduce erosion at the groin's front head better than straight porous groins. In [5], they introduced and compared two numerical schemes, forward time-centered space (FTCS) and backward time-centered space (BTCS), for simulating shoreline evolution on a long-term scale for two beach scenarios. They also presented analytical solutions to shoreline evolution for simple configurations under idealized wave conditions. As a result, BTCS is more suitable than FTCS for simulating shoreline evolution on a long-term scale. In [7], [16], [17], [18], [19], and [20], they developed a one-dimensional shoreline evolution model with a twin-groin structure utilizing two finite difference approaches. The shoreline evolution model is approximated using classic forward time-centered space approaches as well as unconditionally stable Saul'yev finite difference approaches. The model is used to study shoreline erosion and deposition, as well as to forecast the effectiveness of groin system development on a particular beach. In [8], [9], [10], [11], and [12], They employed conditionally stable explicit finite difference approaches to estimate their model results.

In this paper, we introduce the one-dimensional shoreline evolution model, the wave crest impact model to determine the averaged wave crest impact for the left and right sides of the groin structures, the initial and boundary conditions when two types of groin structures are installed, and four wavelengths of the wave crest impact model under consideration. The wave crest impact on the shoreline has been divided into consideration for the left and right sides of the shoreline. Finite difference techniques will be used to approximate the model's solution. We focus on determining the efficiency of four cases of wavelengths in wave crest impact angle and two types of groin structure in shoreline evolution.

II. GOVERNING EQUATION

A. Shoreline evolution model

In a one-dimensional shoreline evolution model, all of the bottom outlines should become parallel while the beach form remains constant and moves toward the land and the sea. Consequently, as the beach reduces and increases, so should the design and volume of the beach level. Sand is moved along the shore on a profile between two clearly specified limit heights, which is the model's core idea. Where there is a difference between the rate of longshore sand transfer on the side of the segment and the associated sand condition, the adjustment in volume is affected. The laws of mass conservation must be regularly modified for the system [5]:

$$\frac{\partial y}{\partial t} = D \frac{\partial^2 y}{\partial x^2}, \quad (1)$$

for all $(x, t) \in (L, T)$, where

$$D = \frac{2Q_0}{D_B + D_C}. \quad (2)$$

where x is the alongshore coordinate (m), y is the shoreline positions (m) and perpendicular to the x -axis, t is time (day), Q_0 is the long-shore sand transport rate amplitude (m^3/day), D_B is the average berm height (m), D_C is the average closure depth (m) and α_0 is the angle between breaking wave crests impact angle and x -axis.

B. Initial and boundary conditions for shoreline evolution model

The initial and boundary conditions of two types of groin structure for the shoreline evolution model

We assumed the initial beach to be parallel to the x -axis.

Assuming that, the angle between the breaking wave crests impact angle and the shoreline is divided symmetrically. The angle between the breaking wave crests impact angle and the left and right areas of the shoreline is α_L , α_R respectively. It follows that the sand transport rate along the shoreline is consistent. The groin structures are added on both sides at $x=0$ and $x=L$ are illustrated in Fig. 1. Under this assumption, the initial condition for I-head and T-head groin structures becomes:

$$y(x, t) = 0, \quad \text{at } t = 0, \quad (3)$$

boundary conditions are also assumed by,

$$\frac{\partial y(x, t)}{\partial x} = -\tan(\alpha_L) \quad \text{at } x = 0, \quad (4)$$

and

$$\frac{\partial y(x, t)}{\partial x} = -\tan(\alpha_R) \quad \text{at } x = L, \quad (5)$$

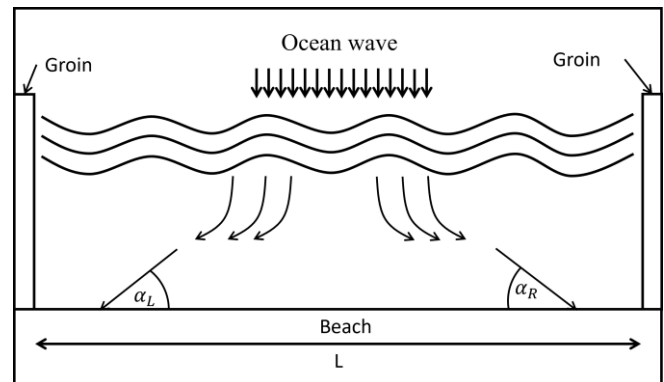


Fig. 1. Initial shoreline with I-head groin structure.

C. Wave crest impact model

To simulate the averaged wave crest impact in the shoreline evolution model, the hydrodynamic model is introduced. [13].

The two-dimensionally unstable water flows into and out of the shoreline can be determined using a system of shallow water equations that account for momentum and mass conservation. The equations for this method should be derived from the depth-averaged Navier-Stokes equations in

the vertical direction, omitting the variables for the effects of friction, surface wind, Coriolis factor, shear stress, and momentum diffusion due to vibration. The continuity equation can then be expressed as follows:

$$\frac{\partial h}{\partial t} + \frac{\partial(uh)}{\partial x} + \frac{\partial(vh)}{\partial y} = 0, \quad (6)$$

and the momentum equations are expressed as below:

$$\frac{\partial(uh)}{\partial t} + \frac{\partial\left(u^2h + \frac{1}{2}gh^2\right)}{\partial x} + \frac{\partial(uvh)}{\partial y} = 0, \quad (7)$$

$$\frac{\partial(uh)}{\partial t} + \frac{\partial(uvh)}{\partial x} + \frac{\partial\left(v^2h + \frac{1}{2}gh^2\right)}{\partial y} = 0, \quad (8)$$

where

$h(x, y, t)$ is the estimated depth from the average sea surface to the seashore bed (m) $h = H + \xi$,

$\xi(x, y, t)$ is the elevation of the sea surface above the average sea level (m),

$H(x, y)$ is the seashore's interpolated bottom topography function (m),

$u(x, y, t)$ is the x -axis velocity direction (m/s),

$v(x, y, t)$ is the y -axis velocity direction (m/s),

g is a gravity constant ($9.8 m/s^2$).

Such time (t) and two space coordinates x and y are the independent variables. Likewise, the conserved quantities are mass, which is proportional to h , and momentum, which is proportional to (uh) and (vh) . As taken with respect to the same term, the partial derivatives are grouped into vectors $(\partial x, \partial y, \partial t)$ and then rewritten as a partial differential hyperbolic equation as follows:

$$U = \begin{pmatrix} h \\ uh \\ vh \end{pmatrix}, F(U) = \begin{pmatrix} uh \\ u^2h + \frac{1}{2}gh^2 \\ uvh \end{pmatrix}, \quad (9)$$

$$G(U) = \begin{pmatrix} vh \\ uvh \\ v^2h + \frac{1}{2}gh^2 \end{pmatrix}. \quad (10)$$

The hyperbolic PDE:

$$\frac{\partial U}{\partial t} + \frac{\partial F(U)}{\partial x} + \frac{\partial G(U)}{\partial y} = 0. \quad (11)$$

D. The initial and boundary condition of 2 types of groin structure for the wave crest impact model

The initial conditions of the shoreline were as follows: the x -axis and y -axis velocity direction as well as the elevation of the water surface, all of which are assumed to be zero: $u = 0, v = 0$ and $\xi = 0$.

Assume that the 2 types of groin structures are not perfect structures to protect waves of water because of its rock

composition, which has large gaps.

The boundary condition was for I-head groin structure as follows: (i) $u = 0, \frac{\partial v}{\partial y} = 0, \xi = f(x, y, t)$ for wave coming, (ii) $\frac{\partial u}{\partial x} = 0, v = 0, \frac{\partial \xi}{\partial x} = 0$ for left and right boundary, (iii) $u = 0, \frac{\partial v}{\partial y} = 0, \frac{\partial \xi}{\partial y} = 0$ for along the beach, (iv) $u = 0, \frac{\partial v}{\partial y} = 0, \frac{\partial \xi}{\partial y} = 0$ for top side of I-head groin structure, and (v) $\frac{\partial u}{\partial x} = 0, v = 0, \frac{\partial \xi}{\partial x} = 0$ for left and right sides of I-head groin structure. The boundary conditions are illustrated in Fig. 2.

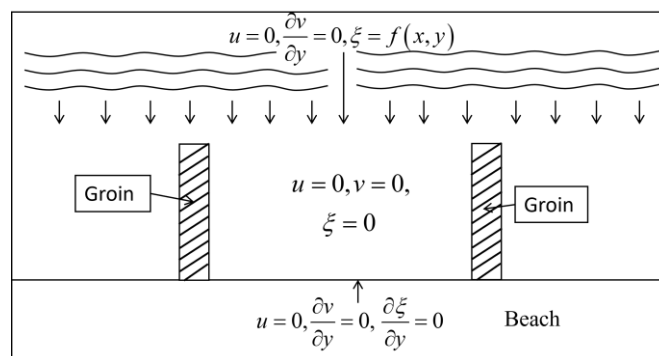


Fig. 2. The I-head Groin initial and boundary conditions.

The boundary condition of T-head groin structure was as follows: (i) $u = 0, \frac{\partial v}{\partial y} = 0, \xi = f(x, y, t)$ for wave coming, (ii) $\frac{\partial u}{\partial x} = 0, v = 0, \frac{\partial \xi}{\partial x} = 0$ for left and right boundary, (iii) $u = 0, \frac{\partial v}{\partial y} = 0, \frac{\partial \xi}{\partial y} = 0$ for along the beach, (iv) $u = 0, \frac{\partial v}{\partial y} = 0, \frac{\partial \xi}{\partial y} = 0$ for top side of T-head groin structure, (v) $u = 0, \frac{\partial v}{\partial y} = 0, \frac{\partial \xi}{\partial y} = 0$ for bottom side of T-head groin structure, and (vi) $\frac{\partial u}{\partial x} = 0, v = 0, \frac{\partial \xi}{\partial x} = 0$ for left and right sides of T-head groin structure. The boundary conditions are illustrated in Fig. 3.

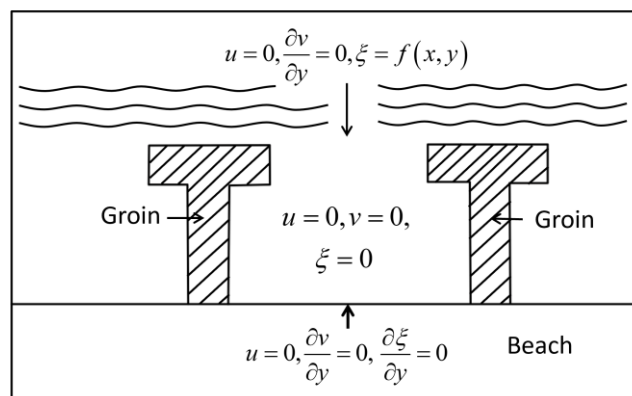


Fig. 3. The T-head groin initial and boundary condition.

III. NUMERICAL TECHNIQUES

A. Grid Spacing

In simulation, we specify that x is in the interval $[0, L]$ and t is in the interval $[0, T]$. We are dividing the x interval into I subintervals, where $I\Delta x = L$, and the t interval into N subintervals, where $N\Delta t = T$. Then we approximate $y(x_i, t_n)$ by y_i^n , at the points $x_i = i\Delta x$ and $t_n = n\Delta t$, where $0 \leq i \leq I$ and $0 \leq n \leq N$.

B. Traditional forward time centered space techniques

The traditional forward time centered space techniques will also be used. We can determine that the finite difference approximation is [14],

$$\frac{\partial y}{\partial t} \cong \frac{y_i^{n+1} - y_i^n}{\Delta t}, \quad (12)$$

$$\frac{\partial y}{\partial x} \cong \frac{y_{i+1}^n - y_{i-1}^n}{2\Delta x}, \quad (13)$$

$$\frac{\partial^2 y}{\partial x^2} \cong \frac{y_{i+1}^n - 2y_i^n + y_{i-1}^n}{(\Delta x)^2}, \quad (14)$$

where $A = \frac{D\Delta t}{(\Delta x)^2}$.

Substituting (12)–(14), in (1), we are obtaining,

$$\frac{y_i^{n+1} - y_i^n}{\Delta t} = D \left(\frac{y_{i+1}^n - 2y_i^n + y_{i-1}^n}{(\Delta x)^2} \right), \quad (15)$$

for $1 \leq i \leq I-1$ and $0 \leq n \leq N-1$. (15), can be written in an explicit form of finite difference as follows,

$$y_i^{n+1} = Ay_{i+1}^n + (1-2A)y_i^n + Ay_{i-1}^n, \quad (16)$$

for $1 \leq i \leq I-1$ and $0 \leq n \leq N-1$.

C. An unconditionally Saulyev finite difference techniques

An unconditionally Saulyev finite difference techniques will also be used. We can determine that the finite difference approximation is [15]

$$\frac{\partial y}{\partial t} \cong \frac{y_i^{n+1} - y_i^n}{\Delta t}, \quad (17)$$

$$\frac{\partial^2 y}{\partial x^2} \cong \frac{y_{i+1}^n - y_i^n - y_i^{n+1} + y_{i-1}^n}{(\Delta x)^2}, \quad (18)$$

where $A = \frac{D\Delta t}{(\Delta x)^2}$.

Substituting (17)–(18), in (1), we are obtaining,

$$\frac{y_i^{n+1} - y_i^n}{\Delta t} = D \left(\frac{y_{i+1}^n - y_i^n - y_i^{n+1} + y_{i-1}^n}{(\Delta x)^2} \right), \quad (19)$$

for $1 \leq i \leq I-1$ and $0 \leq n \leq N-1$. (19), can be written in an explicit form of finite difference as follows,

$$y_i^{n+1} = \frac{1}{(1+A)} \left(Ay_{i+1}^n + (1-A)y_i^n + Ay_{i-1}^n \right), \quad (20)$$

for $1 \leq i \leq I-1$ and $0 \leq n \leq N-1$.

D. Numerical method for the wave crest impact model

The finite difference technique is

$$U_{i,j}^{n+1} = U_{i,j}^n - \frac{\Delta t}{\Delta x} \left(F_{i+\frac{1}{2},j}^{n+\frac{1}{2}} - F_{i-\frac{1}{2},j}^{n+\frac{1}{2}} \right) - \frac{\Delta t}{\Delta y} \left(G_{i,j+\frac{1}{2}}^{n+\frac{1}{2}} - G_{i,j-\frac{1}{2}}^{n+\frac{1}{2}} \right). \quad (21)$$

E. The averaged wave crest impact

We can determine that the wave crest impact is

$$\alpha(x_i, y_j, t) = \tan^{-1} \left(\frac{v(x_i, y_j, t)}{u(x_i, y_j, t)} \right), \quad (22)$$

We assume that the averaged wave crest impact on the left and right sides is assumed by

$$\alpha_L(t) = \frac{\sum_{i=1}^{N_p/2} \alpha(x_i, 0, t)}{N_p/2}, \quad (23)$$

$$\alpha_R(t) = \frac{\sum_{i=N_p/2}^{N_p} \alpha(x_i, 0, t)}{N_p/2}, \quad (24)$$

where N_p is several sample points along the shoreline for wave crest impact.

F. The application of finite difference techniques to the left and right boundary conditions

The traditional forward time centered space technique will also be used. We can determine that the finite difference approximation is,

$$\frac{\partial y}{\partial t} \cong \frac{y_i^{n+1} - y_i^n}{\Delta t}, \quad (25)$$

$$\frac{\partial y}{\partial x} \cong \frac{y_{i+1}^n - y_{i-1}^n}{2\Delta x}, \quad (26)$$

where $A = \frac{D\Delta t}{(\Delta x)^2}$.

Substituting (25) - (26), in (1), we are obtaining,

$$\frac{y_i^{n+1} - y_i^n}{\Delta t} = D \left(\frac{y_{i+1}^n - 2y_i^n + y_{i-1}^n}{(\Delta x)^2} \right), \quad (27)$$

We approximated the substitution of the uncertain value of the left and right boundaries by using the center difference with the specified left and right boundary conditions.

For the left boundary $i = 0$, we are obtaining,

$$y_{-1}^n = y_1^n - 2(\Delta x)(-\tan(\alpha_L)), \quad (28)$$

substituting (29), in (28), we are obtaining,

$$y_i^{n+1} = (1-2A)y_i^n + 2Ay_{i+1}^n - 2A(\Delta x)(-\tan(\alpha_L)). \quad (29)$$

For the right boundary $i = I$, we are obtaining,

$$y_{I+1}^n = y_{I-1}^n + 2(\Delta x)(-\tan(\alpha_R)), \quad (30)$$

substituting (31), in (28), we are obtaining,

$$y_i^{n+1} = 2Ay_{i-1}^n + (1-2A)y_i^n + 2A(\Delta x)(-\tan(\alpha_R)), \quad (31)$$

To approximate the values y_i^n of the solution domain grid points, we will use (29) and (31).

IV. WAVELENGTH SETTING

We assumed wave came in a function of wavelength is $0.5\sin(t_n + \Lambda x_i)$. We considered four case scenarios of wavelengths are $0.5\sin(t_n + 0.01x_i)$, $0.5\sin(t_n + 0.02x_i)$, $0.5\sin(t_n + 0.03x_i)$ and $0.5\sin(t_n + 0.04x_i)$. The consideration shoreline is illustrated in Fig 11, 12.

We will use the finite difference method (21) to estimate the values of the wave crest impact model for all four cases of wavelengths. The results of the wave crest impact model estimation at 10-minute intervals over 1, 5, 10, and 15 years. We will use (23) to obtain the averaged wave crest impact on the left side of groin structures and (24) to obtain the averaged wave crest impact on the right side of groin structures.

The results of the four case wavelengths of the wave crest impact model estimation for the I-head groin structure will be illustrated in Fig. 4. The averaged wave crest impact on the left side and right side of the groin structure are shown in Tables 1 and 2, respectively.

The estimation of the wave crest impact model for the T-head groin structure will be illustrated in Fig. 5. The averaged wave crest impact on the left side and right side of the groin structure are shown in Tables 3 and 4.

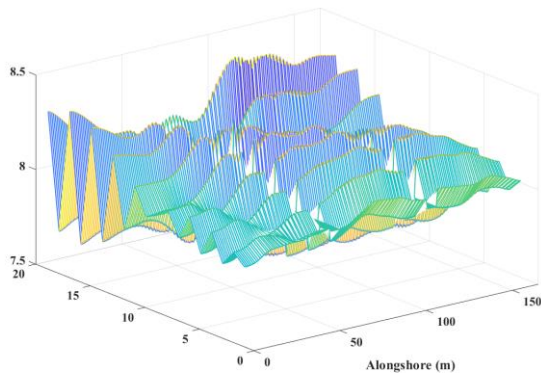


Fig. 4. Wave crest impact in 15 years for the I-head groin when wavelength $0.5\sin(t + 0.01x)$

TABLE I
THE AVERAGED WAVE CREST IMPACT FOR THE LEFT SIDE OF THE I-HEAD GROIN IN 15 YEARS WHEN WAVELENGTH $0.5\sin(t + 0.01x)$

Years	0-10	10-20	20-30	30-40	40-50	50-60
1	0.0635	0.0630	0.0626	0.0621	0.0617	0.0612
5	-0.0684	-0.0690	-0.0697	-0.0703	-0.0710	-0.0717
10	0.1189	0.1187	0.1185	0.1183	0.1181	0.1179
15	-0.0720	-0.0725	-0.0729	-0.0734	-0.0738	-0.0743
Years	...	1390-1400	1400-1410	1410-1420	1420-1430	1430-1440
1	...	0.0078	0.0074	0.0069	0.0064	0.0060
5	...	-0.4073	-0.4162	-0.4254	-0.4350	-0.4449
10	...	0.1287	0.1287	0.1287	0.1286	0.1285
15	...	-0.2531	-0.2565	-0.2600	-0.2636	-0.2672

TABLE II
THE AVERAGED WAVE CREST IMPACT FOR THE RIGHT SIDE OF THE I-HEAD GROIN IN 15 YEARS WHEN WAVELENGTH $0.5\sin(t + 0.01x)$

Years	0-10	10-20	20-30	30-40	40-50	50-60
1	0.0110	0.0105	0.0101	0.0097	0.0092	0.0088
5	0.0026	0.0014	0.0002	-0.0011	-0.0024	-0.0037
10	-0.2291	-0.2310	-0.2330	-0.2350	-0.2371	-0.2392
15	0.0616	0.0613	0.0610	0.0607	0.0604	0.0601
Years	...	1390-1400	1400-1410	1410-1420	1420-1430	1430-1440
1	...	-0.0854	-0.0868	-0.0883	-0.0898	-0.0914
5	...	0.0766	0.0850	0.0934	0.1020	0.1106
10	...	0.4321	0.4213	0.4104	0.3995	0.3886
15	...	0.2286	0.2355	0.2425	0.2495	0.2565

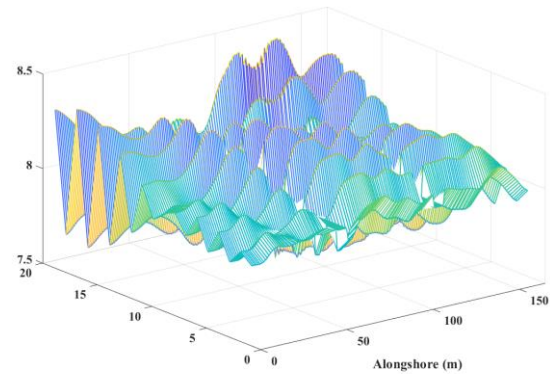


Fig. 5. Wave crest impact in 15 years for the T-head groin when wavelength $0.5\sin(t + 0.01x)$

TABLE III
THE AVERAGED WAVE CREST IMPACT FOR THE LEFT SIDE OF THE T-HEAD GROIN IN 15 YEARS WHEN WAVELENGTH $0.5\sin(t + 0.01x)$

Years	0-10	10-20	20-30	30-40	40-50	50-60
1	0.0872	0.0872	0.0872	0.0872	0.0872	0.0871
5	0.0887	0.0884	0.0881	0.0877	0.0874	0.0871
10	-0.1489	-0.1499	-0.1509	-0.1520	-0.1530	-0.1540
15	0.2571	0.2570	0.2569	0.2568	0.2567	0.2566
Years	...	1390-1400	1400-1410	1410-1420	1420-1430	1430-1440
1	...	0.0635	0.0632	0.0629	0.0626	0.0623
5	...	-0.0675	-0.0730	-0.0789	-0.0852	-0.0919
10	...	-0.5255	-0.5314	-0.5375	-0.6693	-0.6756
15	...	0.3338	0.3359	0.3380	0.3402	0.3424

TABLE IV
THE AVERAGED WAVE CREST IMPACT FOR THE RIGHT SIDE OF THE T-HEAD GROIN IN 15 YEARS WHEN WAVELENGTH $0.5\sin(t + 0.01x)$

Years	0-10	10-20	20-30	30-40	40-50	50-60
1	-0.0267	-0.0274	-0.0281	-0.0288	-0.0295	-0.0302
5	-0.2943	-0.2989	-0.3036	-0.3085	-0.3136	-0.3188
10	-0.0511	-0.0533	-0.0555	-0.0578	-0.0602	-0.0626
15	-0.2271	-0.2292	-0.2314	-0.2336	-0.2359	-0.2382
Years	...	1390-1400	1400-1410	1410-1420	1420-1430	1430-1440
1	...	-0.1712	-0.1735	-0.1758	-0.1781	-0.1805
5	...	0.1759	0.1607	0.1454	0.1299	0.1144
10	...	0.4026	0.4063	0.2844	0.2881	0.2918
15	...	0.2761	0.3926	0.3834	0.3741	0.3649

V. NUMERICAL EXPERIMENT

In this section, we will present the numerical results of the shoreline evolution model for a disappearing beach with I-head and T-head groin structures along the shoreline, as well

as the solution to the idealized problem. To approximate the shoreline evolution model, we will use the traditional forward time centered space techniques (16) and the unconditionally Sauljev finite difference techniques (20). During the experiments, we assumed that the beach (L) was 100 meters long between the groins. The averaged wave crest impact for the left (α_L) and right (α_R) sides of groin structures along the shoreline for I-head groin and T-head groin structures are shown in Table 1-2 and Table 3-4 respectively. The long-shore transport rate (D) for each month [27] is shown in Table 5.

TABLE V
THE LONG-SHORE TRANSPORT RATE

Month	D (m / day)
January	79.4659
February	62.1307
March	5.7869
April	61.4403
May	5.6420
June	5.4716
July	73.0227
August	83.071
September	121.7301
October	372.017
November	96.5710
December	101.1233

The results of approximating the shoreline evolution model for the I-head groin structure are shown in Fig. 6-17 and Table 6, 7, 10, 11, 14, 15, 18 and 19. The approximate of the shoreline evolution model for T-head groin are shown in Fig. 18-29 and Table 8, 9, 12, 13, 16, 17, 20 and 21.

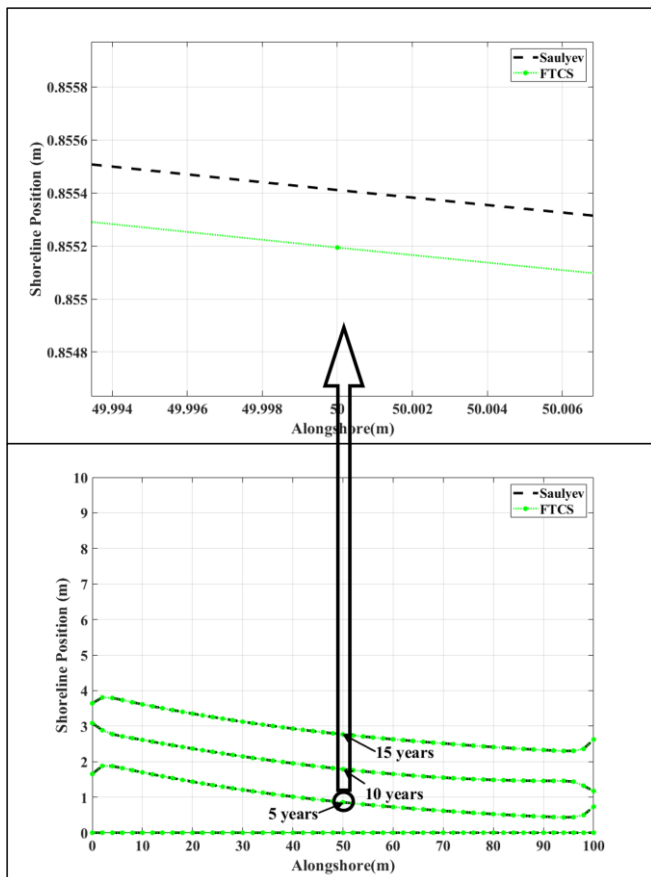


Fig. 6. Shoreline evolution at 5th year for the I-head groin when wavelength $0.5\sin(t + 0.01x)$.

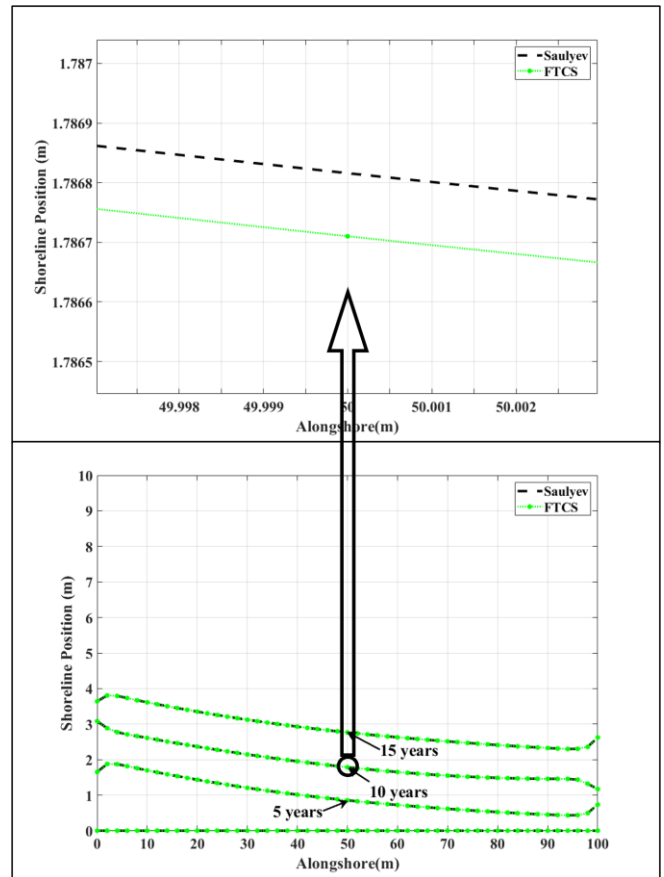


Fig. 7. Shoreline evolution at 10th year for the I-head groin when wavelength $0.5\sin(t + 0.01x)$.

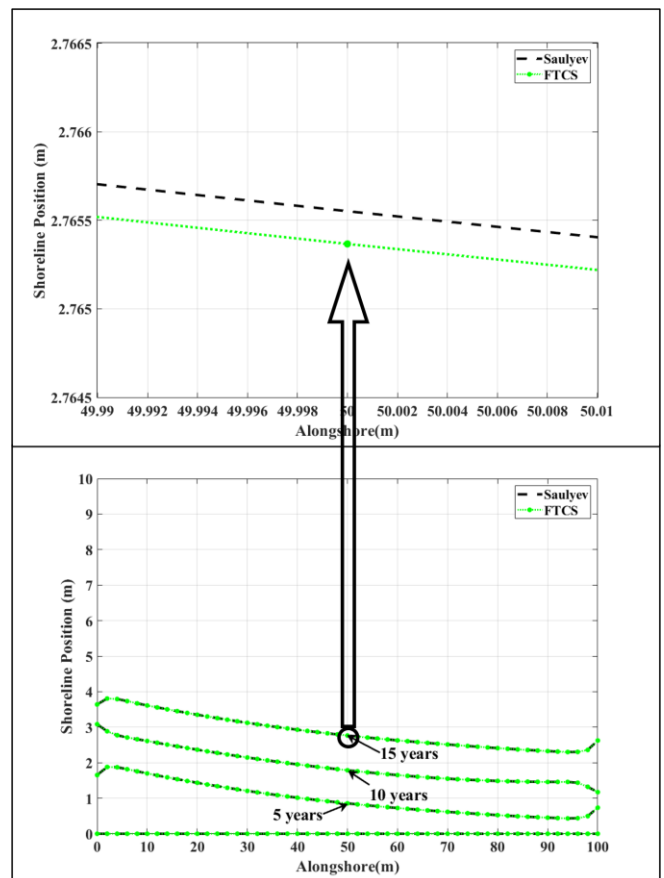


Fig. 8. Shoreline evolution at 15th year for the I-head groin when wavelength $0.5\sin(t + 0.01x)$.

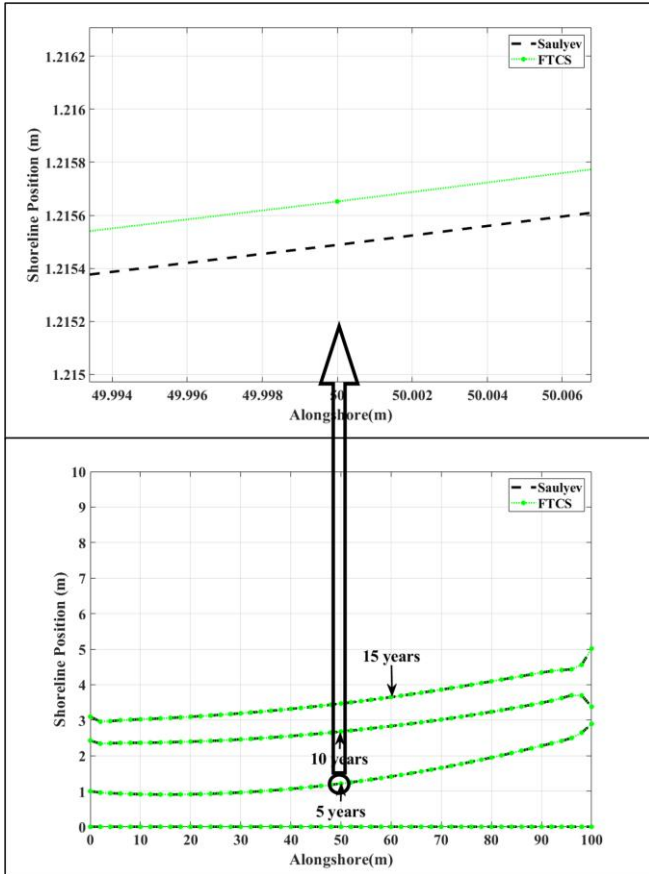


Fig. 9. Shoreline evolution at 5th year for the I-head groin when wavelength $0.5\sin(t + 0.02x)$.

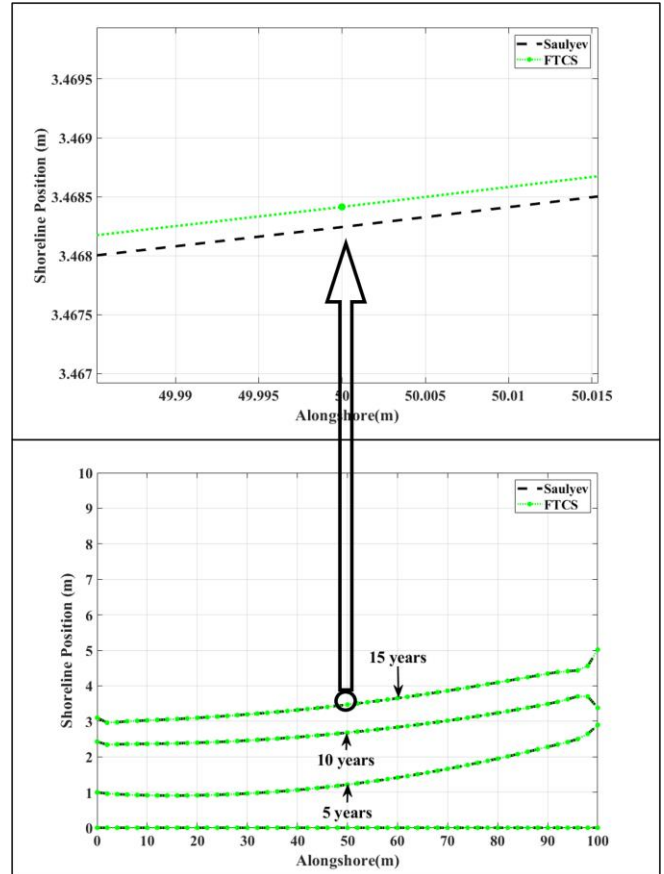


Fig. 11. Shoreline evolution at 15th year for the I-head groin when wavelength $0.5\sin(t + 0.02x)$.

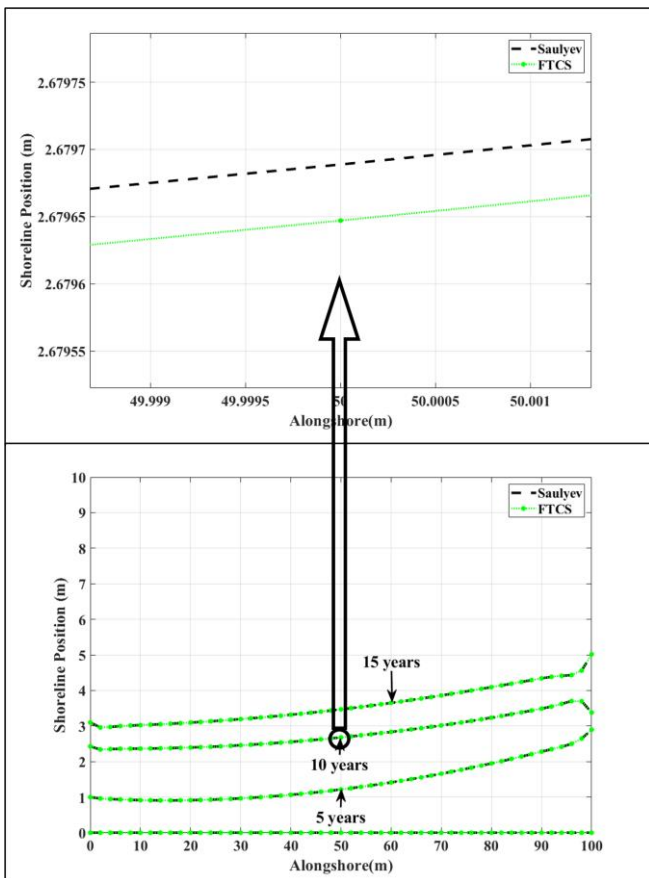


Fig. 10. Shoreline evolution at 10th year for the I-head groin when wavelength $0.5\sin(t + 0.02x)$.

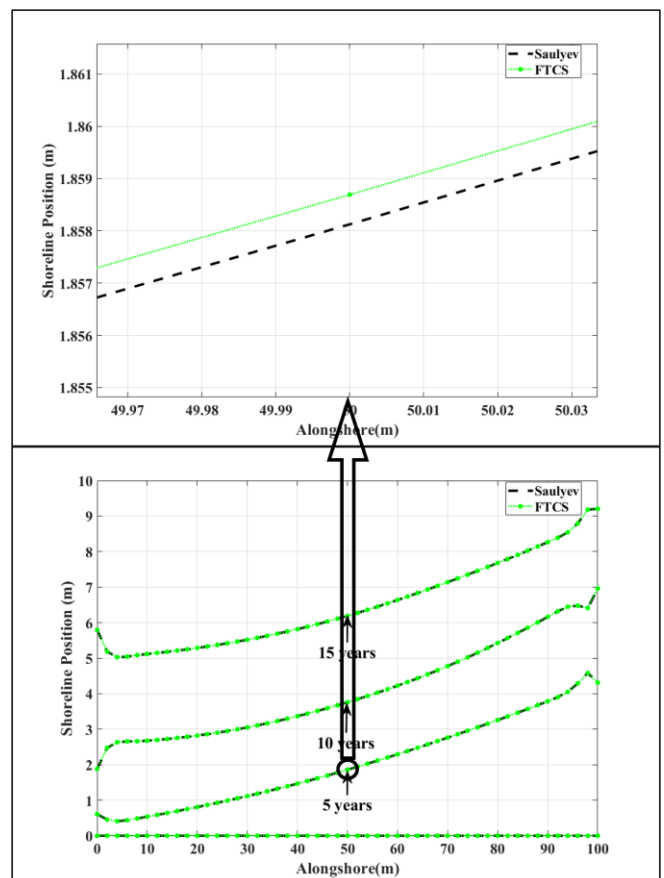


Fig. 12. Shoreline evolution at 5th year for the I-head groin when wavelength $0.5\sin(t + 0.03x)$.

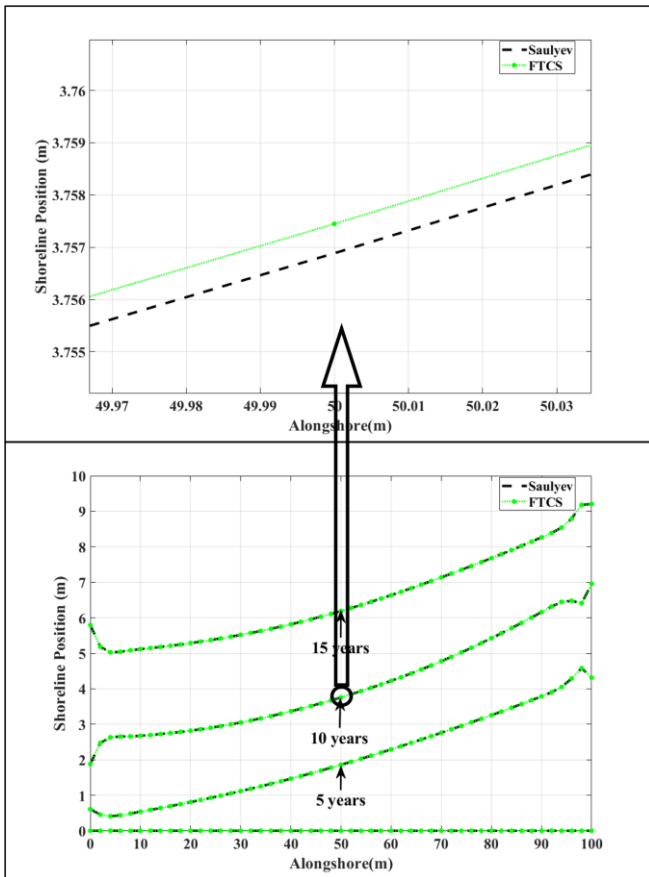


Fig. 13. Shoreline evolution at 10th year for the I-head groin when wavelength $0.5\sin(t + 0.03x)$.

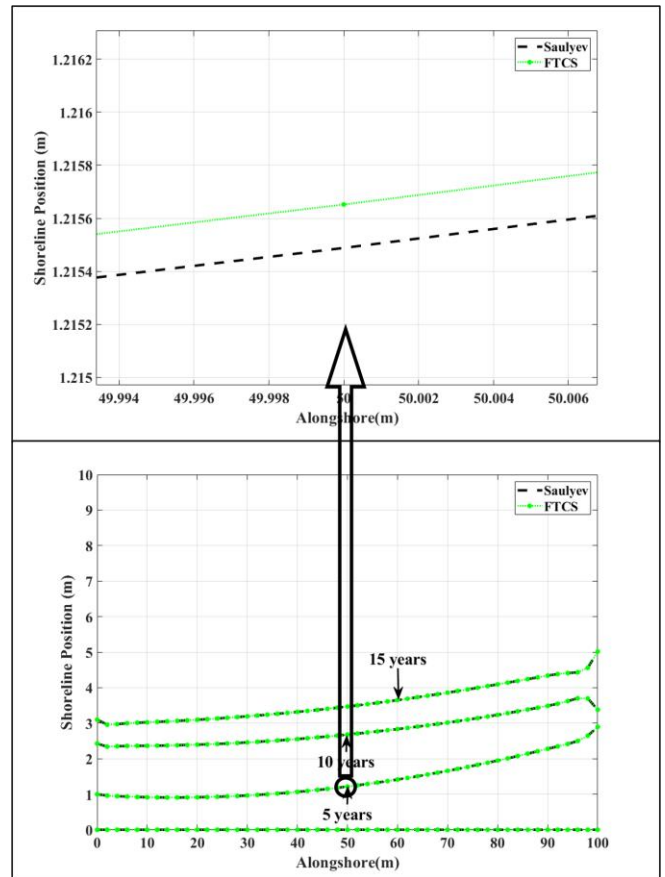


Fig. 15. Shoreline evolution at 5th year for the I-head groin when wavelength $0.5\sin(t + 0.04x)$.

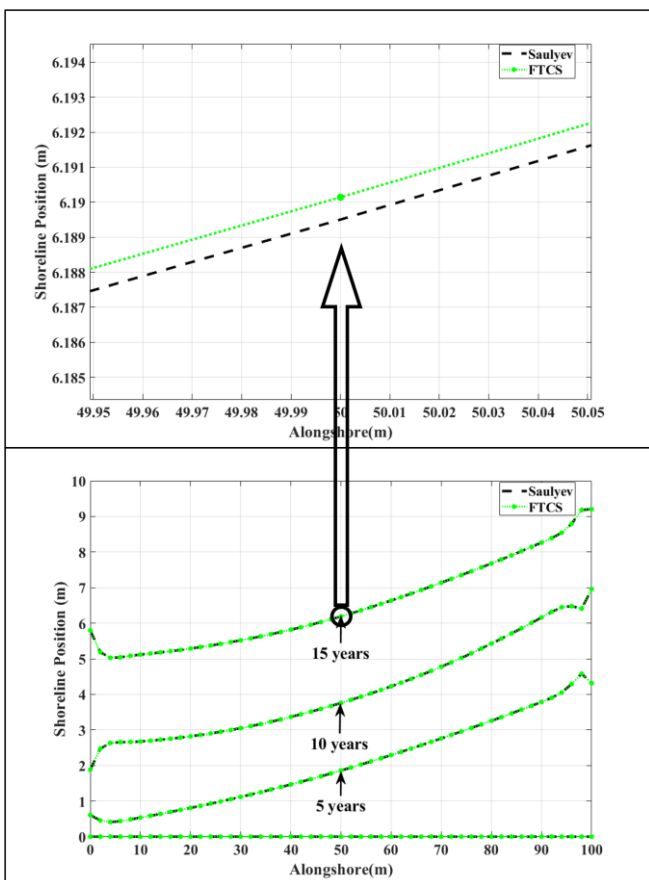


Fig. 14. Shoreline evolution at 15th year for the I-head groin when wavelength $0.5\sin(t + 0.03x)$.

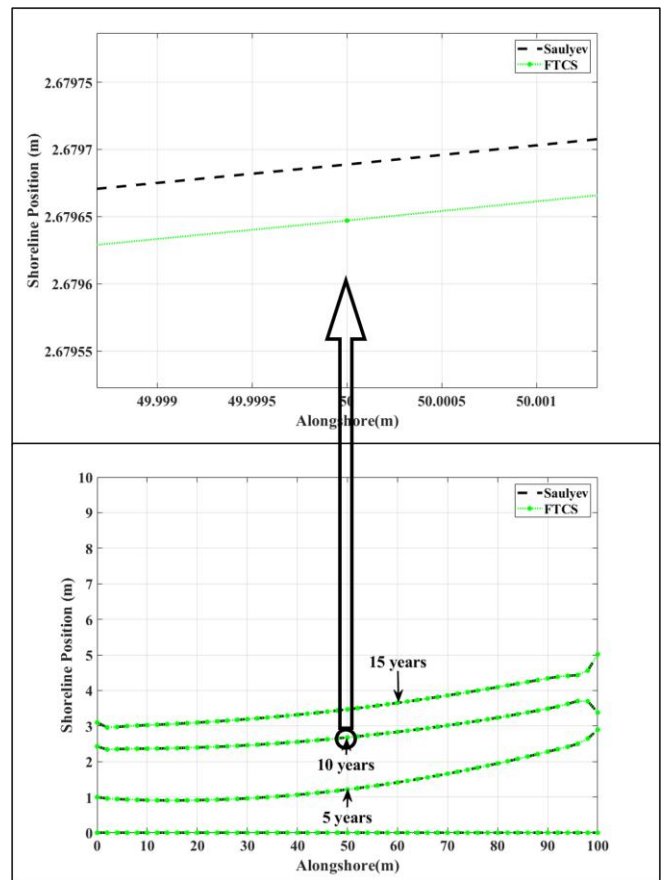


Fig. 16. Shoreline evolution at 10th year for the I-head groin when wavelength $0.5\sin(t + 0.04x)$.

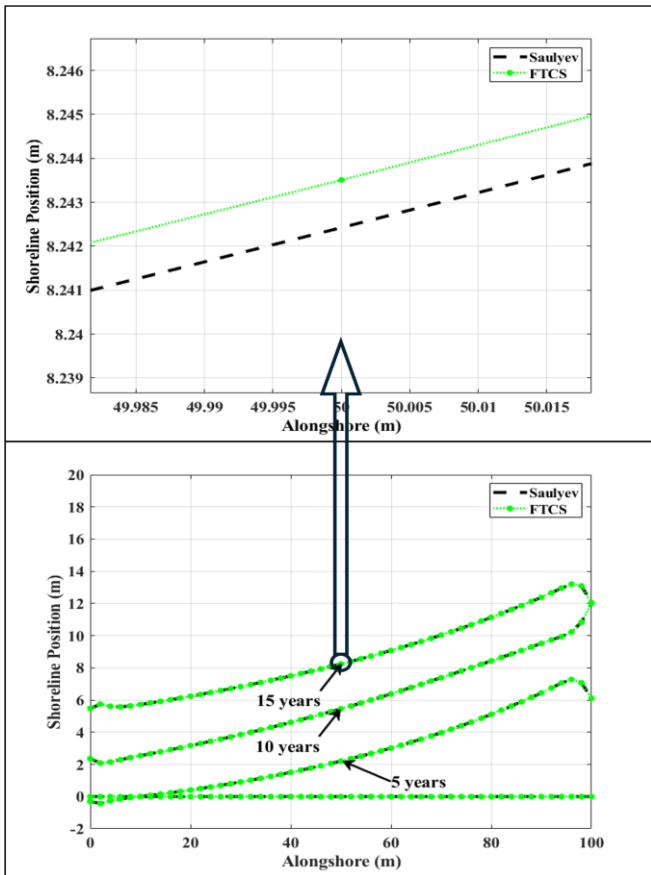


Fig. 17. Shoreline evolution at 15th year for the I-head groin when wavelength $0.5\sin(t + 0.04x)$.

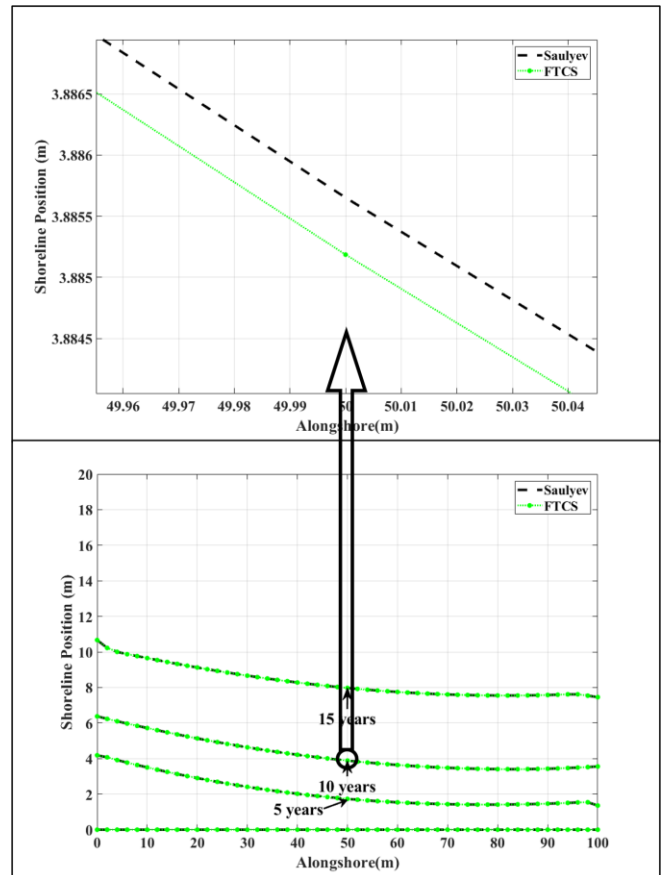


Fig. 19. Shoreline evolution at 10th year for the T-head groin when wavelength $0.5\sin(t + 0.01x)$.

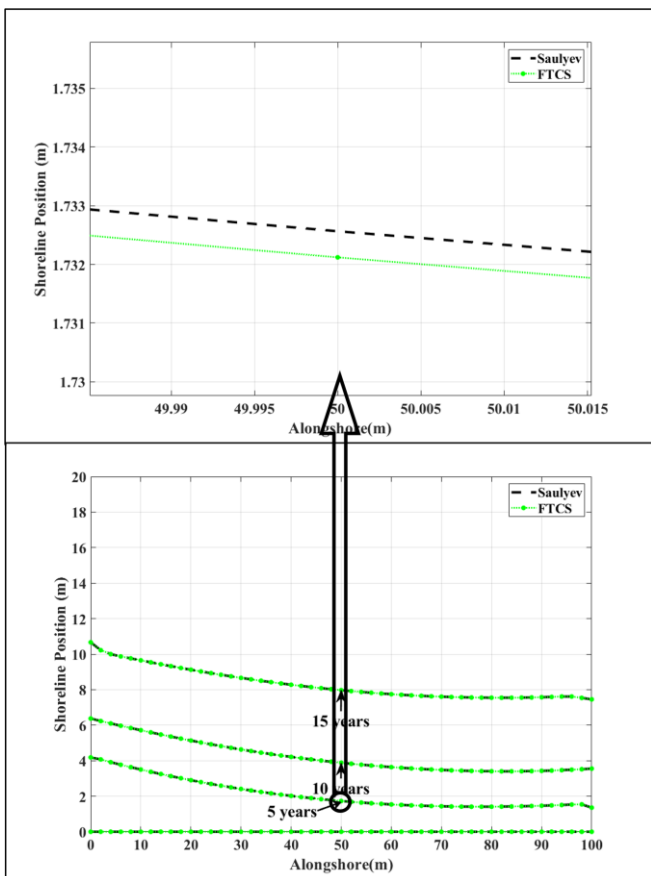


Fig. 18. Shoreline evolution at 5th year for the T-head groin when wavelength $0.5\sin(t + 0.01x)$.

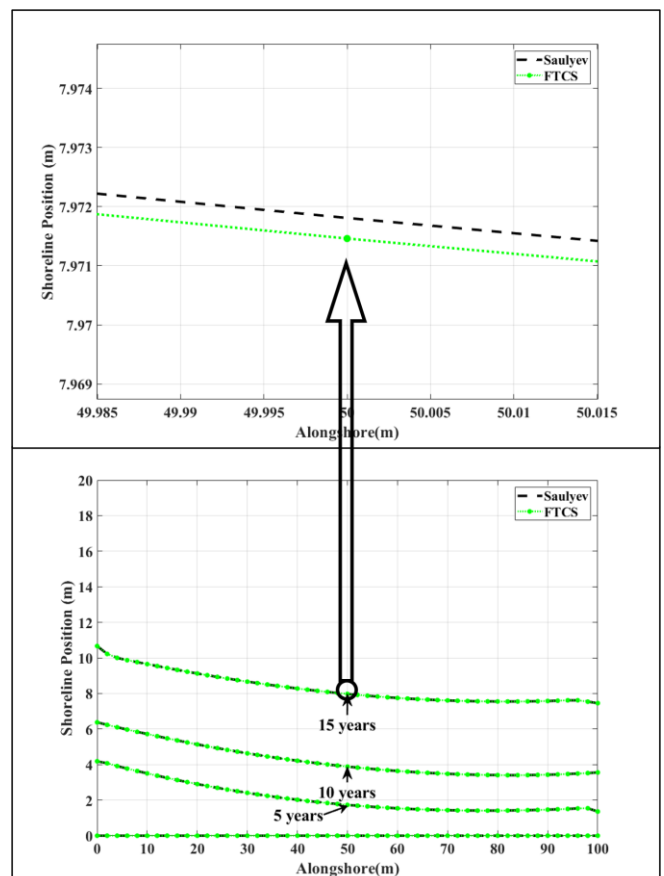


Fig. 20. Shoreline evolution at 15th year for the T-head groin when wavelength $0.5\sin(t + 0.01x)$.

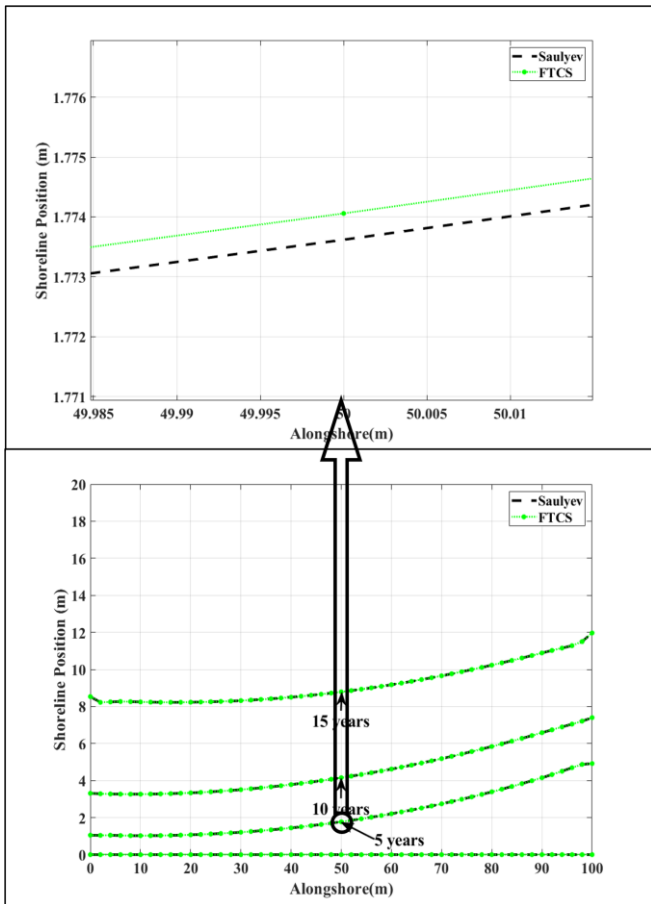


Fig. 21. Shoreline evolution at 5th year for the T-head groin when wavelength $0.5\sin(t + 0.02x)$.

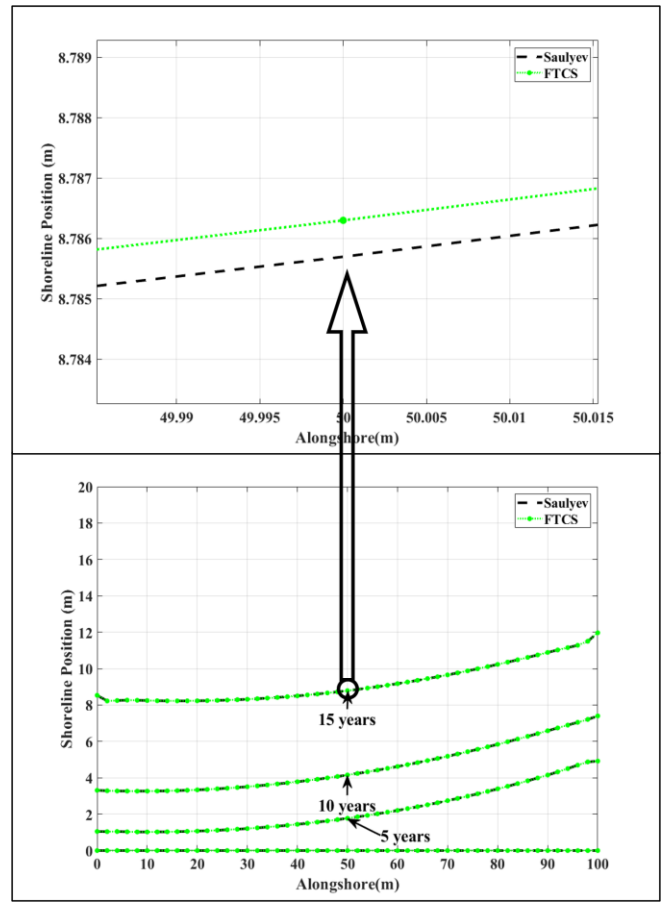


Fig. 23. Shoreline evolution at 15th year for the T-head groin when wavelength $0.5\sin(t + 0.02x)$.

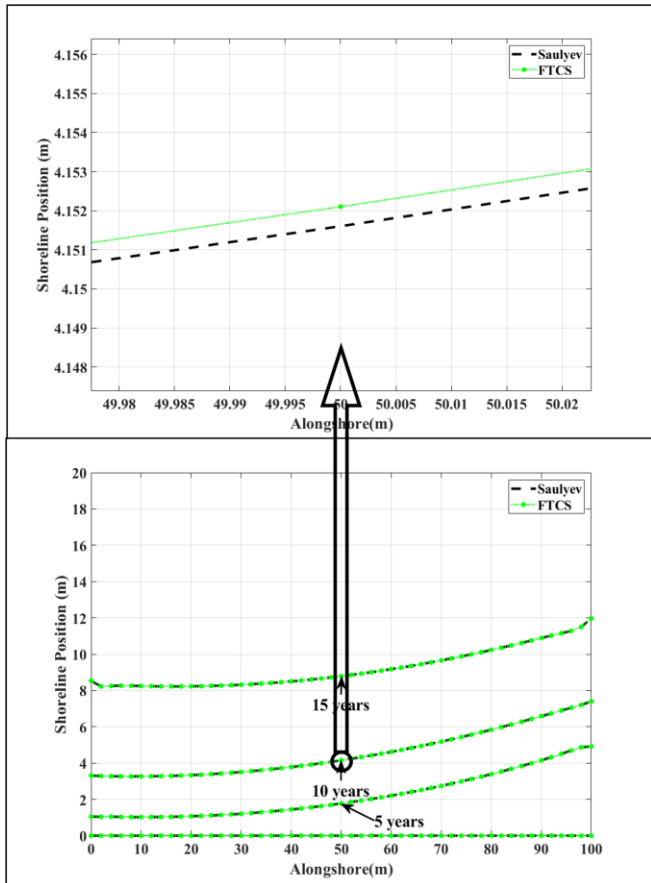


Fig. 22. Shoreline evolution at 10th year for the T-head groin when wavelength $0.5\sin(t + 0.02x)$.

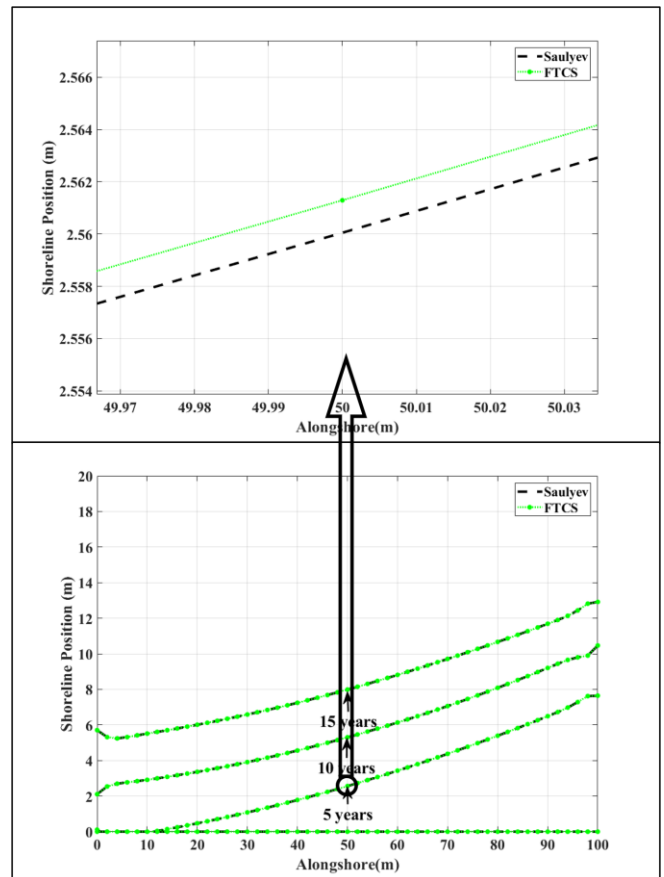


Fig. 24. Shoreline evolution at 5th year for the T-head groin when wavelength $0.5\sin(t + 0.03x)$.

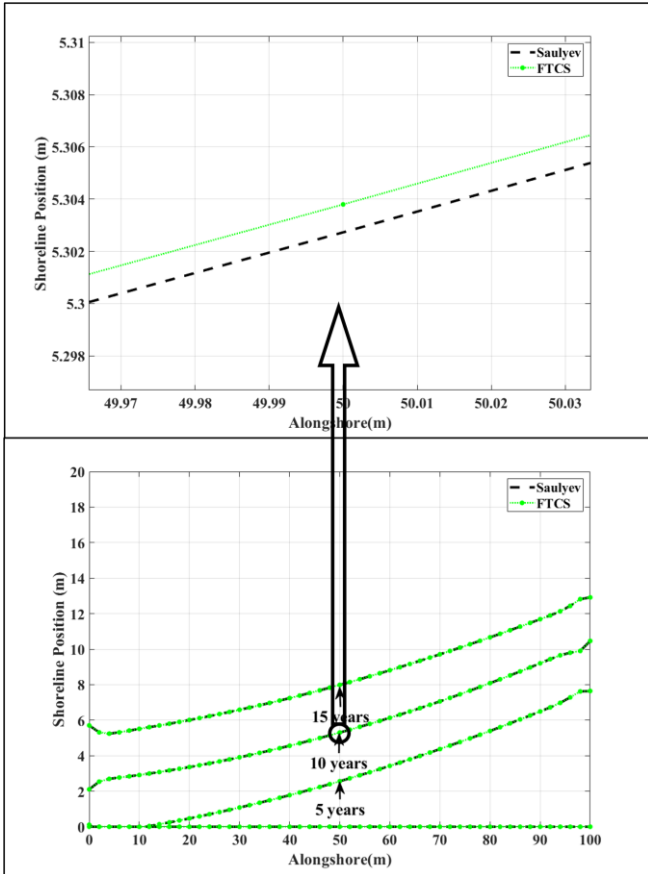


Fig. 25. Shoreline evolution at 10th year for the T-head groin when wavelength $0.5\sin(t + 0.03x)$.

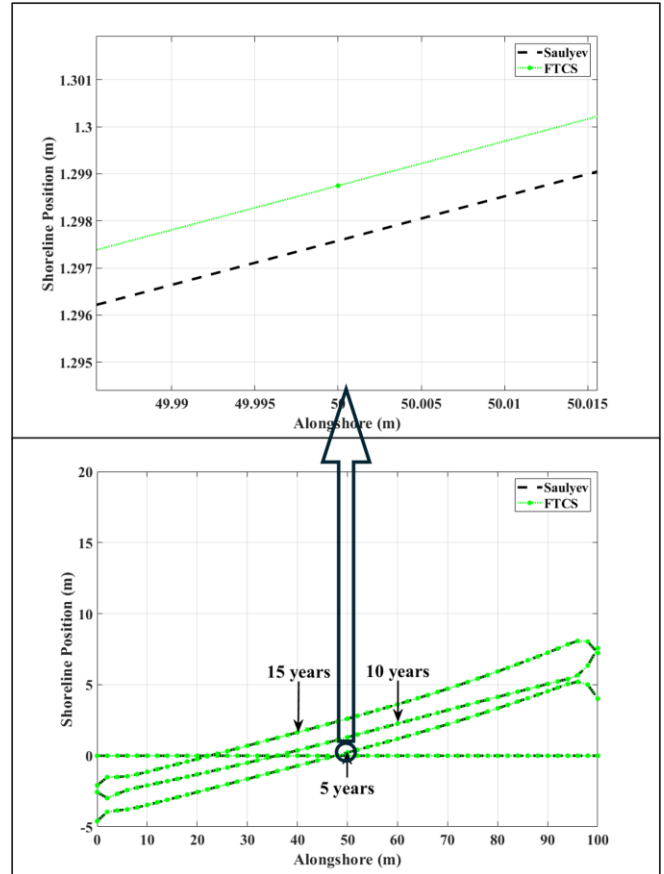


Fig. 27. Shoreline evolution at 5th year for the T-head groin when wavelength $0.5\sin(t + 0.04x)$.

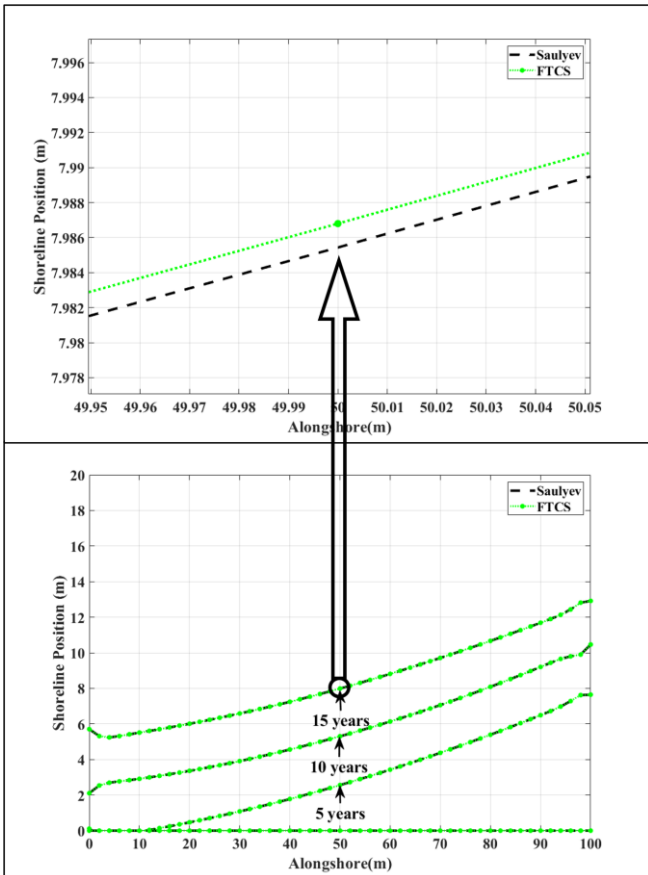


Fig. 26. Shoreline evolution at 15th year for the T-head groin when wavelength $0.5\sin(t + 0.03x)$.

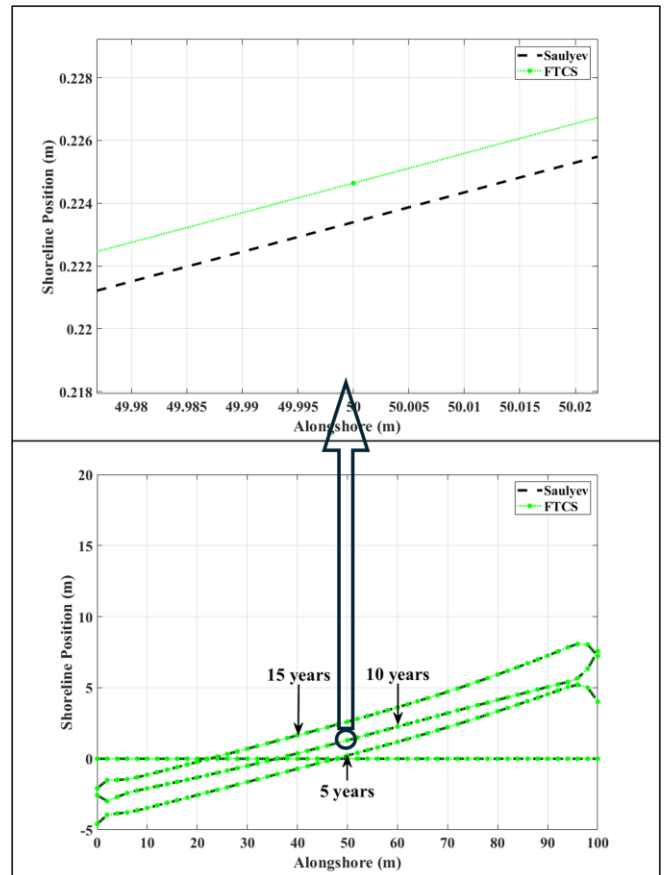


Fig. 28. Shoreline evolution at 10th year for the T-head groin when wavelength $0.5\sin(t + 0.04x)$.

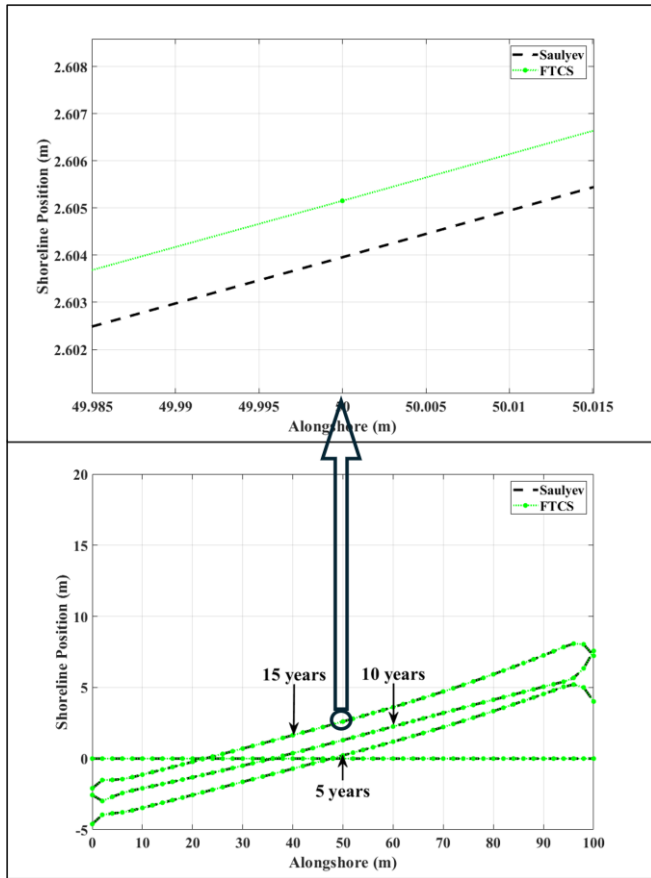


Fig. 29. Shoreline evolution at 15th year for the T-head groin when wavelength $0.5\sin(t + 0.04x)$.

TABLE VI

APPROXIMATED SHORELINE EVOLUTION FOR THE I-HEAD GROIN USING THE TRADITIONAL FORWARD TIME CENTERED SPACE TECHNIQUES WHEN WAVELENGTH $0.5\sin(t + 0.01x)$

Time (Years)	Distance(m)					
	0	20	40	60	80	100
1	0.9941	0.4492	0.1555	0.0180	-0.0508	-0.0840
5	1.6523	1.4345	1.0148	0.7243	0.5244	0.7338
10	3.0839	2.3662	1.9526	1.6516	1.4865	1.1719
15	3.6398	3.3502	2.9288	2.6287	2.4106	2.6247

TABLE VII

APPROXIMATED SHORELINE EVOLUTION FOR THE I-HEAD GROIN USING THE SAULYEV FINITE DIFFERENCE TECHNIQUES WHEN WAVELENGTH $0.5\sin(t + 0.01x)$

Time (Years)	Distance(m)					
	0	20	40	60	80	100
1	0.9945	0.4494	0.1557	0.0181	-0.0508	-0.0841
5	1.6525	1.4348	1.0150	0.7245	0.5247	0.7343
10	3.0837	2.3661	1.9527	1.6517	1.4866	1.1720
15	3.6402	3.3506	2.9290	2.6289	2.4109	2.6252

TABLE VIII

APPROXIMATED SHORELINE EVOLUTION FOR THE T-HEAD GROIN USING THE TRADITIONAL FORWARD TIME CENTERED SPACE TECHNIQUES WHEN WAVELENGTH $0.5\sin(t + 0.01x)$

Time (Years)	Distance(m)					
	0	20	40	60	80	100
1	2.0756	0.9422	0.3720	0.2097	0.3330	0.4301
5	5.1474	3.8837	2.9749	2.4221	2.2241	2.2903
10	7.1689	6.5623	5.6843	5.1434	4.9049	5.2770
15	10.6664	9.1220	8.2785	7.7468	7.5477	7.4545

TABLE IX

APPROXIMATED SHORELINE EVOLUTION FOR THE T-HEAD GROIN USING THE SAULYEV FINITE DIFFERENCE TECHNIQUES WHEN WAVELENGTH $0.5\sin(t + 0.01x)$

Time (Years)	Distance(m)					
	0	20	40	60	80	100
1	2.0762	0.9426	0.3723	0.2098	0.3330	0.4301
5	5.1474	3.8840	2.9754	2.4226	2.2245	2.2908
10	7.1693	6.5630	5.6848	5.1439	4.9055	5.2778
15	10.6663	9.1219	8.2788	7.7471	7.5480	7.4550

TABLE X

APPROXIMATED SHORELINE EVOLUTION FOR THE I-HEAD GROIN USING THE TRADITIONAL FORWARD TIME CENTERED SPACE TECHNIQUES WHEN WAVELENGTH $0.5\sin(t + 0.02x)$

Time (Years)	Distance(m)					
	0	20	40	60	80	100
1	-0.2354	0.1081	0.0836	0.1770	0.4954	1.3974
5	0.9986	0.9142	1.0659	1.4139	1.9478	2.8976
10	2.4266	2.3953	2.5542	2.8335	3.2344	3.3788
15	3.1008	3.0971	3.3171	3.6497	4.0931	5.0172

TABLE XI

APPROXIMATED SHORELINE EVOLUTION FOR THE I-HEAD GROIN USING THE SAULYEV FINITE DIFFERENCE TECHNIQUES WHEN WAVELENGTH $0.5\sin(t + 0.02x)$

Time (Years)	Distance (m)					
	0	20	40	60	80	100
1	-0.2357	0.1081	0.0835	0.1769	0.4951	1.3971
5	0.9988	0.9142	1.0658	1.4137	1.9476	2.8974
10	2.4266	2.3952	2.5542	2.8336	3.2346	3.3788
15	3.1009	3.0971	3.3170	3.6494	4.0927	5.0170

TABLE XII

APPROXIMATED SHORELINE EVOLUTION FOR THE T-HEAD GROIN USING THE TRADITIONAL FORWARD TIME CENTERED SPACE TECHNIQUES WHEN WAVELENGTH $0.5\sin(t + 0.02x)$

Time (Years)	Distance(m)					
	0	20	40	60	80	100
1	-0.3997	-0.0156	0.1200	0.4631	1.3382	3.0257
5	2.0882	1.9957	2.4174	3.2399	4.4675	6.2704
10	5.2645	5.1770	5.5275	6.2421	7.3156	8.3335
15	8.5325	8.2307	8.5004	9.1719	10.2295	11.9670

TABLE XIII

APPROXIMATED SHORELINE EVOLUTION FOR THE T-HEAD GROIN USING THE SAULYEV FINITE DIFFERENCE TECHNIQUES WHEN WAVELENGTH $0.5\sin(t + 0.02x)$

Time (Years)	Distance (m)					
	0	20	40	60	80	100
1	-0.4001	-0.0158	0.1197	0.4626	1.3376	3.0251
5	2.0881	1.9954	2.4169	3.2394	4.4670	6.2700
10	5.2643	5.1766	5.5271	6.2418	7.3153	8.3331
15	8.5321	8.2303	8.4998	9.1712	10.2289	11.9664

TABLE XIV

APPROXIMATED SHORELINE EVOLUTION FOR THE I-HEAD GROIN USING THE TRADITIONAL FORWARD TIME CENTERED SPACE TECHNIQUES WHEN WAVELENGTH $0.5\sin(t + 0.03x)$

Time (Years)	Distance(m)					
	0	20	40	60	80	100
1	-0.0903	-0.0446	0.0895	0.3925	1.0751	2.9663
5	0.6098	0.8091	1.4667	2.2933	3.2557	4.3112
10	1.8799	2.8208	3.3657	4.2239	5.4253	6.9597
15	5.7954	5.2876	5.8170	6.6363	7.6782	9.2039

TABLE XV
APPROXIMATED SHORELINE EVOLUTION FOR THE I-HEAD GROIN USING THE SUALYEV FINITE DIFFERENCE TECHNIQUES WHEN WAVELENGTH $0.5\sin(t + 0.03x)$

Time (Years)	Distance(m)					
	0	20	40	60	80	100
1	-0.0901	-0.0447	0.0893	0.3922	1.0749	2.9663
5	0.6090	0.8082	1.4661	2.2928	3.2556	4.3110
10	1.8796	2.8207	3.3651	4.2233	5.4244	6.9590
15	5.7949	5.2868	5.8164	6.6357	7.6780	9.2036

TABLE XVI
APPROXIMATED SHORELINE EVOLUTION FOR THE T-HEAD GROIN USING THE TRADITIONAL FORWARD TIME CENTERED SPACE TECHNIQUES WHEN WAVELENGTH $0.5\sin(t + 0.03x)$

Time (Years)	Distance(m)					
	0	20	40	60	80	100
1	-1.4156	-0.7042	-0.0665	0.6404	2.0799	4.9916
5	0.1105	0.4694	1.7794	3.4279	5.3927	7.6430
10	2.1081	3.3628	4.5613	6.1344	8.0849	10.4632
15	5.7067	6.0107	7.2438	8.8126	10.6655	12.9144

TABLE XVII
APPROXIMATED SHORELINE EVOLUTION FOR THE T-HEAD GROIN USING THE SUALYEV FINITE DIFFERENCE TECHNIQUES WHEN WAVELENGTH $0.5\sin(t + 0.03x)$

Time (Years)	Distance(m)					
	0	20	40	60	80	100
1	-1.4154	-0.7046	-0.0674	0.6393	2.0790	4.9911
5	0.1093	0.4678	1.7782	3.4266	5.3916	7.6418
10	2.1078	3.3622	4.5603	6.1333	8.0836	10.4621
15	5.7056	6.0091	7.2424	8.8113	10.6646	12.9135

TABLE XVIII
APPROXIMATED SHORELINE EVOLUTION FOR THE I-HEAD GROIN USING THE TRADITIONAL FORWARD TIME CENTERED SPACE TECHNIQUES WHEN WAVELENGTH $0.5\sin(t + 0.04x)$

Time (Years)	Distance(m)					
	0	20	40	60	80	100
1	-0.9673	-0.3797	-0.0057	0.4468	1.3996	2.9295
5	-0.2970	0.4101	1.5087	3.0157	5.1134	6.1132
10	2.3564	3.1690	4.6118	6.3840	8.4343	11.9978
15	5.4803	6.2371	7.5001	9.0816	11.1392	12.0469

TABLE XIX
APPROXIMATED SHORELINE EVOLUTION FOR THE I-HEAD GROIN USING THE SUALYEV FINITE DIFFERENCE TECHNIQUES WHEN WAVELENGTH $0.5\sin(t + 0.04x)$

Time (Years)	Distance(m)					
	0	20	40	60	80	100
1	-0.9680	-0.3803	-0.0061	0.4463	1.3990	2.9287
5	-0.2978	0.4094	1.5079	3.0149	5.1119	6.1113
10	2.3551	3.1677	4.6106	6.3827	8.4333	11.9970
15	5.4781	6.2351	7.4988	9.0807	11.1379	12.0452

TABLE XX
APPROXIMATED SHORELINE EVOLUTION FOR THE T-HEAD GROIN USING THE TRADITIONAL FORWARD TIME CENTERED SPACE TECHNIQUES WHEN WAVELENGTH $0.5\sin(t + 0.04x)$

Time (Years)	Distance(m)					
	0	20	40	60	80	100
1	-2.9709	-1.3919	-0.3780	0.3191	1.4169	2.9464
5	-4.6020	-2.5578	-0.7109	1.1897	3.3375	4.0121
10	-2.5624	-1.3169	0.3759	2.2516	4.1354	7.5685
15	-2.0897	-0.2259	1.6421	3.6170	5.9260	7.2267

TABLE XXI
APPROXIMATED SHORELINE EVOLUTION FOR THE T-HEAD GROIN USING THE SUALYEV FINITE DIFFERENCE TECHNIQUES WHEN WAVELENGTH $0.5\sin(t + 0.04x)$

Time (Years)	Distance(m)					
	0	20	40	60	80	100
1	-2.9717	-1.3928	-0.3788	0.3183	1.4160	2.9454
5	-4.6033	-2.5592	-0.7123	1.1885	3.3358	4.0101
10	-2.5635	-1.3177	0.3749	2.2503	4.1344	7.5675
15	-2.0912	-0.2275	1.6407	3.6159	5.9246	7.2248

The approximated shoreline area in year 15 of approximating the shoreline evolution model for the I-head and T-head groin structures for four cases of wavelengths is shown in table 22.

TABLE XXII
APPROXIMATED SHORELINE AREA IN YEAR 15 OF APPROXIMATING THE SHORELINE EVOLUTION MODEL FOR THE I-HEAD AND T-HEAD GROIN STRUCTURE FOR FOUR CASES OF WAVELENGTHS

Wavelength	Area (m ²)	
	I-Head Groin Structure	T-Head Groin Structure
1	287.5063	830.7850
2	358.4159	919.4715
3	648.0829	832.6448
4	865.2342	282.7154

Comparing I-head and T-head groin structure for each wavelength as shown in Fig 30–37.

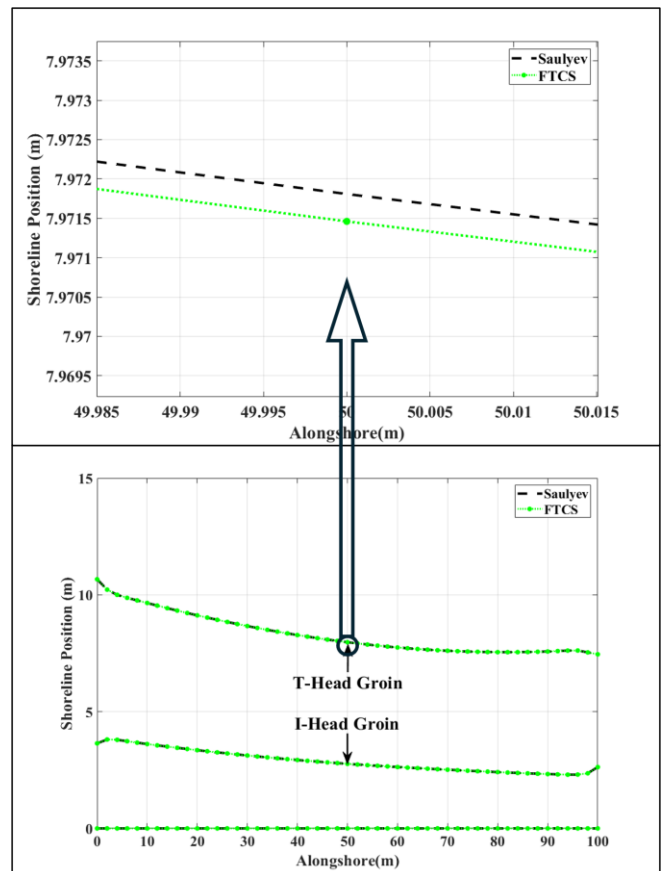


Fig. 30. The shoreline evolution compares I-head and T-head groin zoom in T-head groin when wavelength $0.5\sin(t + 0.01x)$.

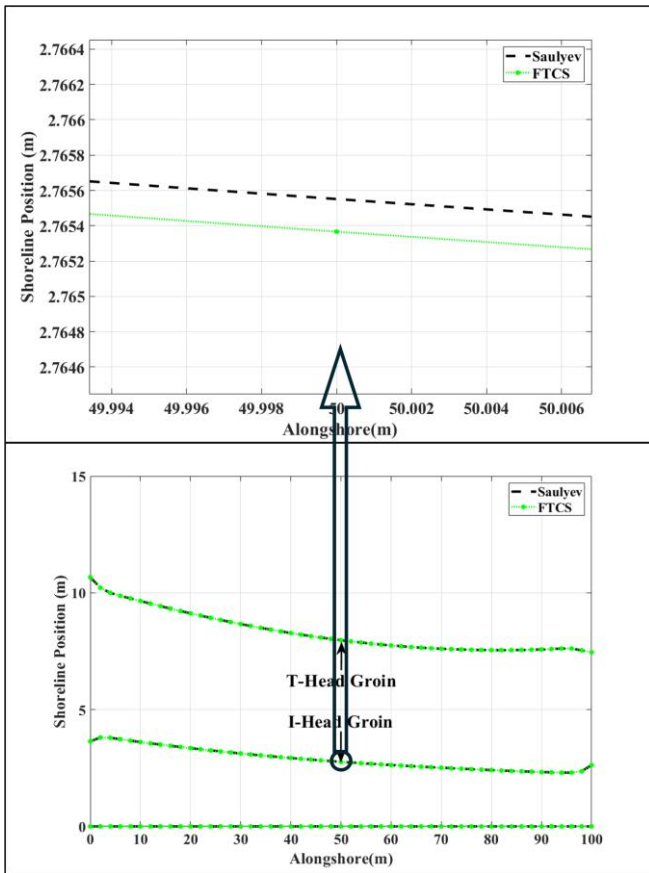


Fig. 31. The shoreline evolution compares I-head and T-head groin zoom in I-head groin when wavelength $0.5\sin(t + 0.01x)$.

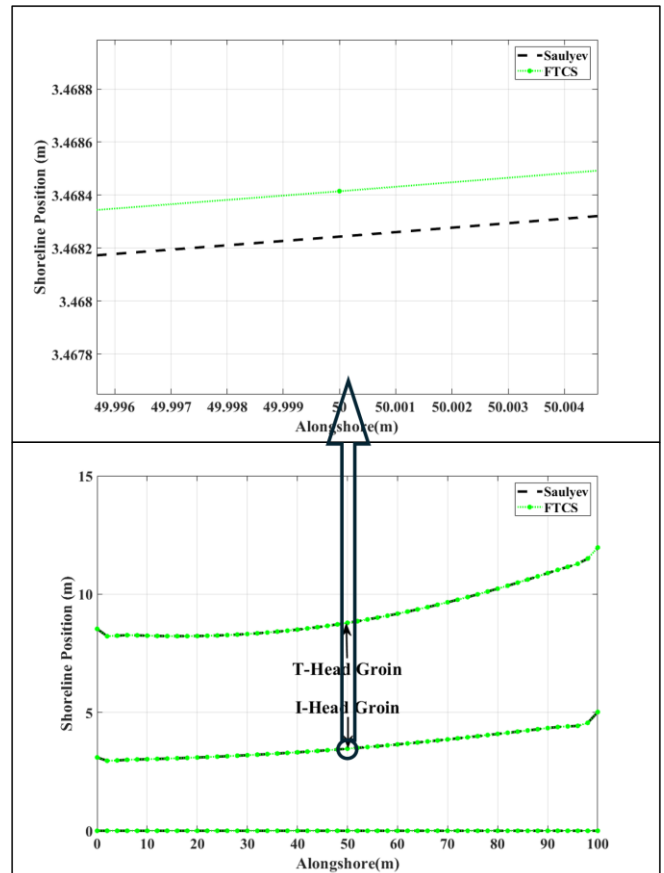


Fig. 33. The shoreline evolution compares I-head and T-head groin zoom in I-head groin when wavelength $0.5\sin(t + 0.02x)$.

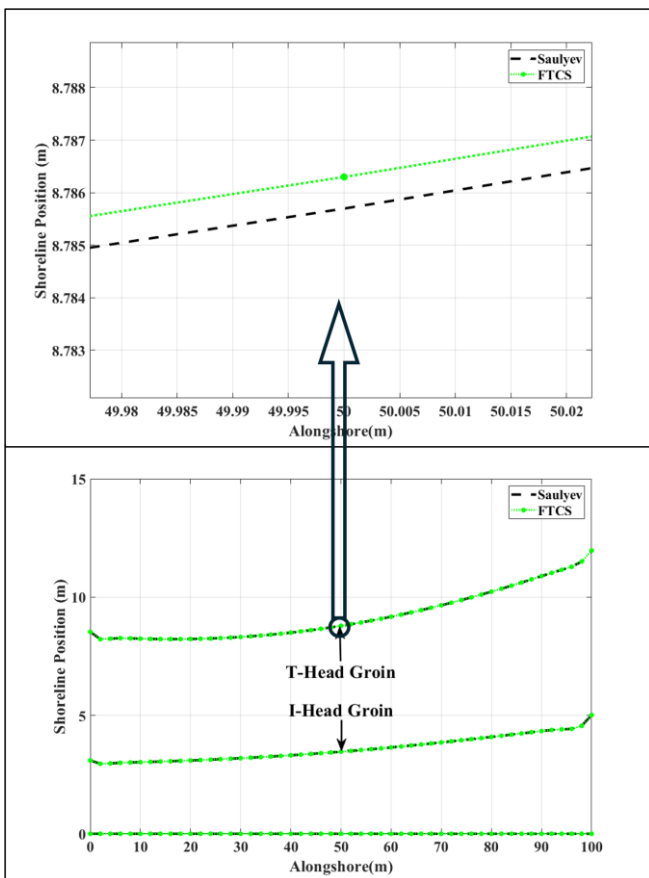


Fig. 32. The shoreline evolution compares I-head and T-head groin zoom in T-head groin when wavelength $0.5\sin(t + 0.02x)$.

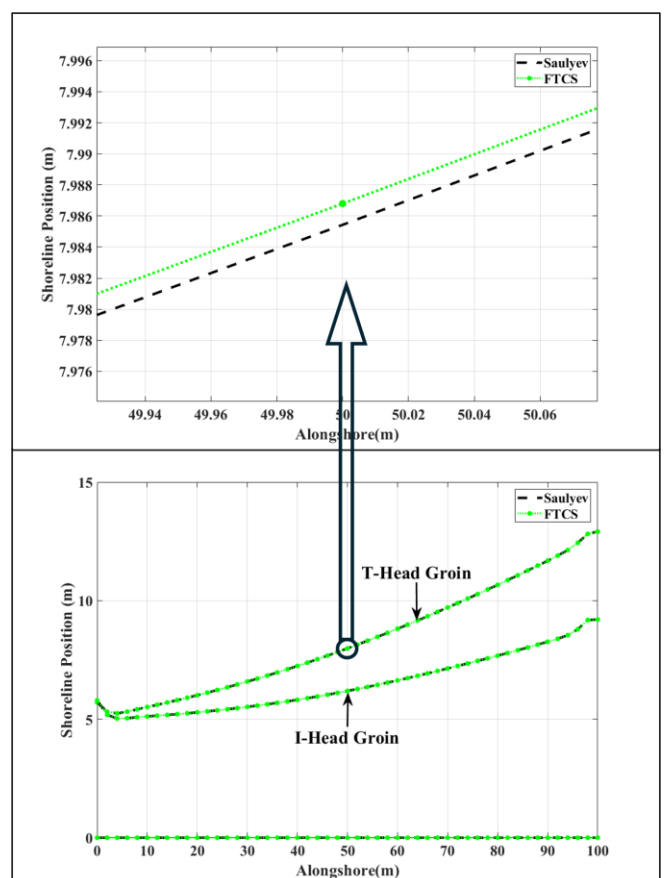


Fig. 34. The shoreline evolution compares I-head and T-head groin zoom in T-head groin when wavelength $0.5\sin(t + 0.03x)$.

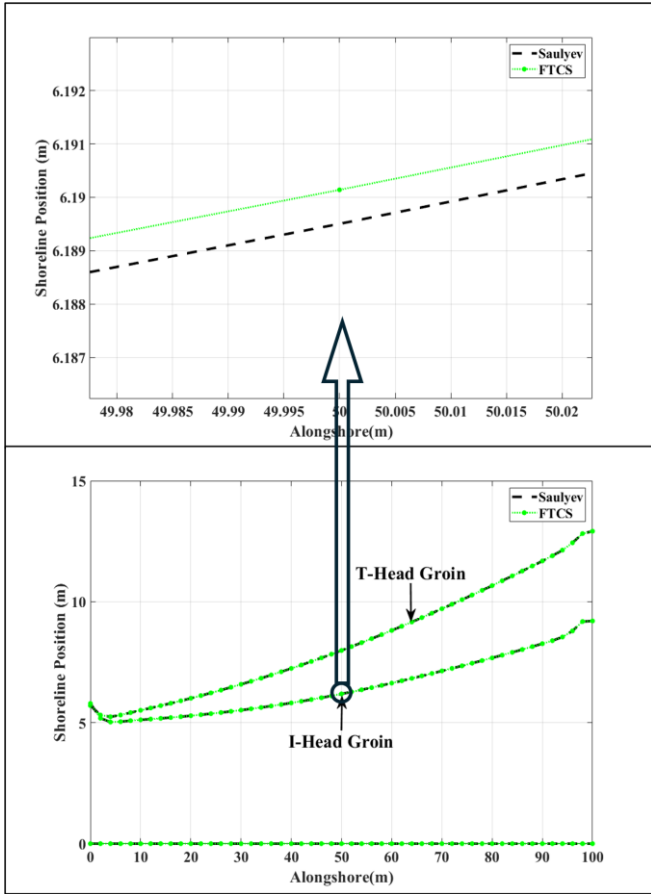


Fig. 35. The shoreline evolution compares I-head and T-head groin zoom in I-head groin when wavelength $0.5\sin(t+0.03x)$.

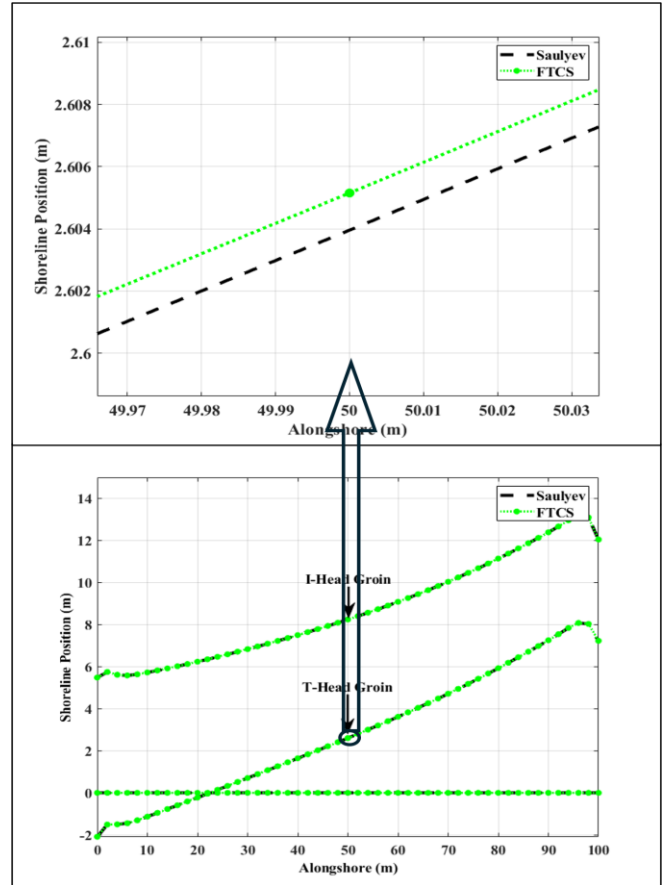


Fig. 37. The shoreline evolution compares I-head and T-head groin zoom in T-head groin when wavelength $0.5\sin(t+0.04x)$.

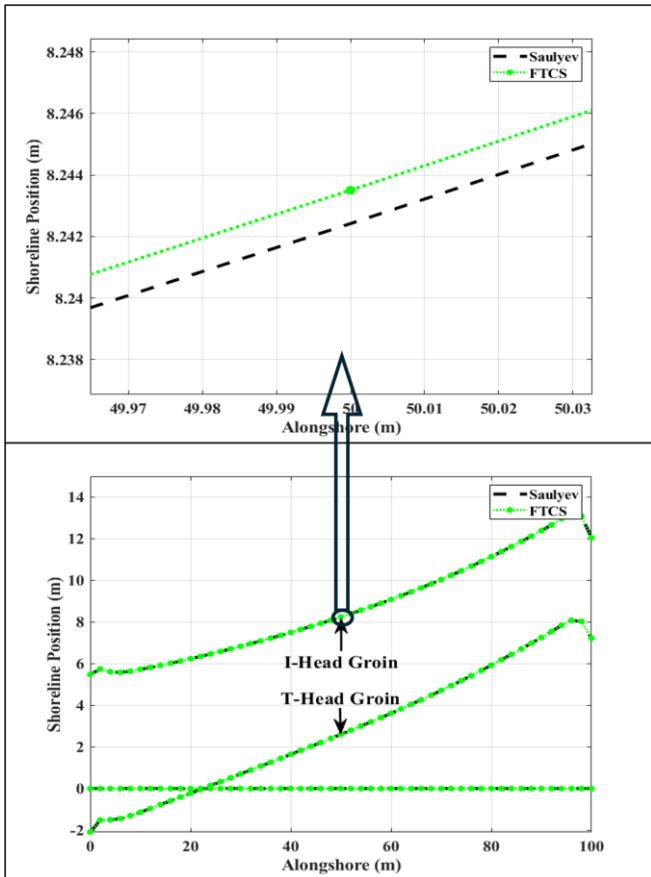


Fig. 36. The shoreline evolution compares I-head and T-head groin zoom in I-head groin when wavelength $0.5\sin(t+0.04x)$.

VI. DISCUSSION

In this paper, we used the wave crest impact model to obtain the approximate averaged wave crest impact obtained by (29). As shown in Table 1-4, this approximate averaged wave crest impact was performed by dividing it into the averaged wave crest impact for the left (α_L) and the right (α_R) sides of the shoreline for each wavelength.

We used two numerical techniques, the traditional forward time centered space techniques (FTCS) (16), and the unconditionally Sauljev finite difference techniques (20), to approximate the shoreline evolution for I-head groin and T-head groin structures.

Tables 6–9 and Fig. 6–8, 18, 19, and 20 show the approximated shoreline evolution for wavelength $0.5\sin(t+0.01x)$ over a 15-year period for I-head and T-head groin installations, respectively. According to the results obtained in the 15th year, the greatest approximate shoreline distance for I-head groin structures on the left groin is 3.6402 meters, and the right groin is 2.6252 meters. The approximate shoreline has obtained beach area is 287.5063 m^2 . The greatest approximate shoreline distance for T-head groin structures is the right groin, which has the greatest approximate distance of 10.6664 meters, while the left groin has a distance of 7.4550 meters. The approximate shoreline has obtained beach area is 830.7850 m^2 .

Tables 10–13 and Fig. 9–11, 21, 22, and 23 show the approximated shoreline evolution for wavelength $0.5\sin(t+0.02x)$ over a 15-year period for I-head and T-head groin installations. According to the results obtained in

the 15th year, the greatest approximate shoreline distance for I-head groin structures on the left groin is 5.0172 meters, and the right groin is 3.3171 meters. The approximate shoreline has obtained beach area is 358.4159 m^2 . The greatest approximate shoreline distance for T-head groin structures is the right groin, which has the greatest approximate distance of 11.9670 meters, while the left groin has a distance of 8.5004 meters. The approximate shoreline has obtained beach area is 919.4715 m^2 .

Tables 14–17 and Fig. 12–14, 24, 25, and 26 show the approximated shoreline evolution for wavelength $0.5\sin(t+0.03x)$ over a 15-year period for I-head and T-head groin installations, respectively. According to the results obtained in the 15th year, the greatest approximate shoreline distance for I-head groin structures on the left groin is 9.2039 meters, and the right groin is 5.8170 meters. The approximate shoreline has obtained beach area is 648.0829 m^2 . The greatest approximate shoreline distance for T-head groin structures is the right groin, which has the greatest approximate distance of 12.9144 meters, while the left groin has a distance of 7.2438 meters. The approximate shoreline has obtained beach area is 832.6448 m^2 .

Tables 18–21 and Fig. 15–17, 27, 28, and 29 show the approximated shoreline evolution for wavelength $0.5\sin(t+0.04x)$ over a 15-year period for I-head and T-head groin installations, respectively. According to the results obtained in the 15th year, the greatest approximate shoreline distance for I-head groin structures on the left groin is 5.4803 meters, and the right groin is 12.0469 meters. The approximate shoreline has obtained beach area is 865.2342 m^2 . The greatest approximate shoreline distance for T-head groin structures is the right groin, which has lost beach area at the lost approximate distance of -2.0912 meters, while the left groin has obtained beach area at a distance of 7.2267 meters. The approximate shoreline has obtained beach area is 282.7154 m^2 .

Fig 30–37 show the approximated shoreline evolution compared between I-head and T-head groin structures at wavelengths $0.5\sin(t+0.01x)$, $0.5\sin(t+0.02x)$, $0.5\sin(t+0.03x)$, and $0.5\sin(t+0.04x)$, respectively.

In wavelength $0.5\sin(t+0.01x)$, the approximated shoreline evolution of the T-head groin structure is longer than the I-head groin structure. The longest distance between the T-head groin and the I-head groin is 7.0262 meters. The T-head groin has obtained a beach area greater than the I-head groin by 543.2728 m^2 .

In wavelength $0.5\sin(t+0.02x)$, the approximated shoreline evolution of the T-head groin structure is longer than the I-head groin structure. The longest distance between the T-head groin and the I-head groin is 6.9498 meters. The T-head groin has obtained a beach area greater than the I-head groin by 561.0556 m^2 .

In wavelength $0.5\sin(t+0.03x)$, the approximated shoreline evolution of the T-head groin structure is longer than the I-head groin structure. The longest distance between the T-head groin and the I-head groin is 3.7105 meters. The T-head groin has obtained a beach area greater than the I-head groin by 184.5619 m^2 .

And wavelength $0.5\sin(t+0.04x)$, the approximated shoreline evolution of the I-head groin structure is longer than the T-head groin structure. The longest distance

between the I-head groin and the T-head groin is 4.8202 meters. The I-head groin has obtained a beach area greater than the T-head groin by 582.5188 m^2 .

Both numerical approaches approximate shoreline evolutions in two types of groin structures considered to be compatible.

VII. CONCLUSION

In this paper, we have presented a shoreline evolution model for a shoreline with two groin structures, namely the I-head groin and T-head groin, installed on the left and right sides, respectively. The left boundary condition is consistence of the average wave crest impact for the left sides (α_L), and the right boundary condition is consistence of the average wave crest impact for the right sides (α_R). To estimate the values of the average wave crest impact for the left side (α_L) and the average wave crest impact for the right side (α_R) for both types of groins, we utilized the wave crest impact model while considering three different wavelengths. The initial condition setting approach and boundary condition techniques are discussed, as well as the structural impacts of the I-head groin and T-head groin.

We used the forward time centered space techniques and unconditionally stable Saul'yev finite differential techniques to estimate shoreline evolution. The estimated shoreline evolution was consistent with the wave crest impact model for I-head and T-head groin structures and four cases of wavelengths. Compared to the approximated shoreline evolution of the I-head groin structure and the T-head groin structure, the approximated shoreline evolution of the T-head groin structure is longer than the I-head groin structure for three cases of wavelengths.

As a result, the approximated shoreline evolution for wavelengths 1, 2, and 4 appears to be quite similar for both the I-head and T-head groin structures on both the left and right sides. However, for wavelength 3, there is a notable and significant difference in the approximated shoreline evolution between the left and right sides for both the I-head and T-head groin structures. The approximated shoreline evolution for wavelengths 1, 2, and 3 T-head groin structures has obtained more beach area than I-head groin structures. But in wavelength 4, the I-head groin structure has obtained more beach area than the T-head groin. The approximated shoreline evolution for the T-head groin configuration exhibited larger values than that of the I-head groin configuration across three wavelengths. One wavelength, the I-head groin configuration, showed higher values than the T-head groin configuration.

The wavelength has affected T-head and I-head, and there is a significant difference in the approximated shoreline. When the wavelength increases, the T-head groin has less than the approximated shoreline, but the I-head groin has more than the approximated shoreline.

REFERENCES

- [1] T. Beuzen, I. L. Turner, C. E. Blenkinsopp, A. Atkinson, F. Flocard, and T.E. Baldock, "Physical model study of beach profile evolution by sea level rise in the presence of seawalls," *Coastal Engineering*, vol. 136, pp. 172–182, 2018.
- [2] M. D'Anna, D. Idier, B. Castelle, S. Vitousek, and G. Le Cozannet, "Reinterpreting the Bruun Rule in the Context of Equilibrium

- Shoreline Models," *Journal of Marine Science and Engineering*, 9, 974, 22 pages, 2021.
- [3] G. Cannata, M. Tamburrino, and F. Gallerano, "3D Numerical Simulation of the Interaction between Waves and a T-Head Groin Structure," *Journal of Marine Science and Engineering*, 8, 227, 21 pages, 2020
- [4] Dalrino, R. Herdianto, and D. B. Silitonga, "Study of groin structures effectiveness for against abrasion in Padang Beach," *IOP Conf. Series: Earth and Environmental Science*, 708, 012035, 2021.
- [5] Subiyanto, Mohammad Fadhli Ahmad, M. Mamat, and M. L. Husain, "Comparison of Numerical Method for Forward and Backward Time Centered Space for Long-Term Simulation of Shoreline Evolution," *Applied Mathematical Sciences*, Vol. 7, no. 104, 5165 - 5173, 2013.
- [6] E. Fatimaha, Zouhrawaty, A. Ariffa, and T. B. Aulia, "The influence of single zigzag type porous groin in the change of beach profile," *Procedia Engineering*, 125, pp. 257 – 262, 2015.
- [7] P. Unyapoti, and N. Pochai, "A Shoreline Evolution Model with a Twin Groins Structure using Unconditionally Stable Explicit Finite Difference Techniques," *Engineering Letters*, vol. 29, no. 1, pp. 288-296, 2021.
- [8] K. Suebyat, and N. Pochai, "A Numerical Simulation of a Three-dimensional Air Quality Model in an Area Under a Bangkok Sky Train Platform Using an Explicit Finite Difference Scheme," *IAENG International Journal of Applied Mathematics*, vol. 47, no. 4, pp. 471-476, 2017.
- [9] T. Sutardi, L. Wang, M. C. Paul, and N. Karimi, "Numerical Simulation Approaches for Modelling a Single Coal Particle Combustion and Gasification," *Engineering Letters*, vol. 26, no. 2, pp. 257-266, 2018.
- [10] L. Li, Z. Wei, and Q. Huang, "A Numerical Method for Solving Fractional Variational Problems by the Operational Matrix Based on Chelyshkov Polynomials," *Engineering Letters*, vol. 28, no. 2, pp. 486-491, 2020.
- [11] P. Othata and N. Pochai, "A Mathematical Model of Salinity Control in a River with an Effect of Internal Waves using Two Explicit Finite Difference Methods," *Engineering Letters*, vol 29, no 2, pp.689-696, 2021.
- [12] W. Kraychang, and N. Pochai, "A Simple Numerical Model for Water Quality Assessment with Constant Absorption around Nok Phrao Island of Trang River," *Engineering Letters*, vol. 28, no. 3, pp. 912-922, 2020.
- [13] W. Kraychang and N. Pochai, "Numerical Treatment to a Water-Quality Measurement Model in an Opened-Closed Reservoir," *Thai Journal of Mathematics*, vol.13, pp. 775-788, 2015.
- [14] A. R. Mitchell, "Computational methods in partial differential equations," John Wiley & Sons Ltd. London, 1969.
- [15] N. Pochai, "Unconditional stable numerical techniques for a water-quality model in a non-uniform flow stream," *Advances in Difference Equations*, vol. 2017, Article ID 286, 13 pages, 2017.
- [16] Pidok Unyapoti and Pochai, N., "A Combination of A Shoreline Evolution Model and A Wave Crest Model on T-Head Groin Structures With the Breaking Wave Effect", *IAENG International Journal of Computer Science*, Vol 50, No 2 (2023), pp. 347-358.
- [17] Pidok Unyapoti and Pochai, N., "A Shoreline Evolution Model With the Wavelength Effect of Breaking Waves on Groin Structures", *IAENG International Journal of Computer Science*, Vol 49, No 3 (2022), pp. 683-694.
- [18] Pidok Unyapoti and Pochai, N., "A Shoreline Evolution Model with a Groin Structure under Non-Uniform Breaking Wave Crest Impact", *Computation*, *Computation* 2021, 9(4), 42, (2021).
- [19] Surasak Manilam and Pochai, N., "A Non-Dimensional Mathematical Model of Shoreline Evolution with a Groin Structure Using an Unconditionally Stable Explicit Finite Difference Technique", *IAENG International Journal of Applied Mathematics*, Vol 52, No 2 (2022), pp. 473-481.
- [20] Surasak Manilam and Pochai, N., "An Unconditionally Stable Explicit Finite Difference Method for a Non-Dimensional Mathematical Model of Shoreline Evolution with a Twin Groins Structure", *Engineering Letters*, Vol 32, No 2 (2024), pp. 296-304.